TAMPERE UNIVERSITY OF TECHNOLOGY

GIULIA GUIDETTI

PHOTOINDUCED ELECTRON TRANSFER AT THE INTERFACE OF SEMICONDUCTOR AND ORGANIC DONOR-ACCEPTOR LAYER

Master's Thesis

Examiner: Prof. Nikolai V. Tkachenko
Examiner and topic approved by the Faculty Council of the Faculty of Science and Bioengineering on
4 September 2013

Abstract

TAMPERE UNIVERSITY OF TECHNOLOGY
Master Degree Programme in Science and Engineering
GUIDETTI, GIULIA: Photoinduced electron transfer at the interface of semiconductor and organic donor-acceptor layer
Master of Science Thesis: 50 pages, 6 appendix pages
Examiner: Professor Nikolai V. Tkachenko
Keywords: photo-induced electron transfer, porphyrin-fullerene dyad, perylene diimide-fullerene dyad, secondary semiconductor acceptor layer, organic monolayer

This work investigates the electron transfer process (ET) at the interface between organic donor-acceptor dyads and semiconductor layers. The main goal was to identify possible combinations of organic dyads and semiconductors to be used in molecular heterojunction organic solar cells. The chosen donor acceptor pairs were porphyrin-fullerene (**PC_{60}**) and perylene diimide-fullerene (**$PDIC_{60}$**) whereas the studied semiconductors were zinc oxide (**ZnO**) and titanium dioxide (**TiO_2**), with alumina (**Al_2O_3**) being the insulator and reference layer. Free-based porphyrin (**CPTPP**) was initially used to study the formation of monolayers.

Spectroscopic studies were carried out to characterize the organic compounds both in solution and as monolayers on different surfaces. The organic monolayer absorption was studied by means of Langmuir-Blodgett (LB) deposition on flat glass substrates and on glass substrates covered by a thin spin-coated **ZnO** layer. Subsequent self-assembled monolayers (SAM) were prepared by dipping method on the same **ZnO** layer and their quality was compared to that of the LB ones. Photo-voltage measurements were carried out, by means of time-resolved Maxwell displacement charge (TRMDC) method, to study the vectorial electron transfer process in the organic layer and between the organic and semiconductor layers. Three different sets of samples were appositely prepared for these measures. An **Al_2O_3** layer was deposited via atomic-layer-deposition (ALD) on **ITO** supports and served as insulating and reference layer with no electron transfer activity. Additional layers of either **ZnO** or **TiO_2** were deposited via ALD on top of the **Al_2O_3** layer to yield two other sets of samples. SAM monolayers of the organic dyads were then deposited on each set and then covered with insulating LB ODA layers.

The preparation of **$PDIC_{60}$** containing samples was satisfactory only on **ZnO** substrate whereas the one of **PC_{60}** on all substrates. Spectroscopic measurements were carried out to characterize the samples and confirm the presence of each molecular layer. TRMDC measures revealed the formation of a charge separated state in the active layer and the following charge recombination process in each sample. In particular the effect of the additional semiconductor layers was characterized. **ZnO** serves as efficient secondary electron acceptor as concluded from ten folds increase of the photo-voltage response of the **PC_{60}** SAM on **ZnO** as compared to that on **Al_2O_3**. For SAMs on **TiO_2** the response was somewhat lower in intensity as compared to **Al_2O_3** samples. For both semiconductors long-lived charge separated states were observed, further confirming the oxide role as secondary electron acceptors. Despite of the observed sample degradation, these structures were considered as promising for organic photovoltaic applications.

Preface

I would like to thank my supervisors Professor Nikolai V. Tkachenko and Dr. Carlo S. Casari. To both of them I am grateful for their belief in me and for giving me the opportunity to carry out this Thesis work. In particular I am obliged to Professor Nikolai V. Tkachenko for the constructive discussions and wise suggestions related both to the practical work and to the theoretical one. To Dr. Carlo S. Casari I would like to express my gratitude for all his help and support.

I am very grateful to Kirsi Huttunen and to Hanna Sarenpää for their constant help and patience. They have been passionate guides for the work always stimulating me to improve. I am truly indebted to Dr. Vladimir Chukharev for his help during the measurements. I am also thankful to all the colleagues from the Department of Chemistry and Bioengineering for the pleasant working environment.

A constant motivation came from my friends Amira, Linda, Lucia and Roberto. Without your cheerful presence it would have been more difficult.

To my parents, Paola and Mauro, my deepest gratitude for always being close.

The research work presented in this Thesis was carried out at the Department of Chemistry and Bioengineering, Tampere University of Technology during the year 2013.

Tampere, August 2013

Giulia Guidetti

Table of Contents

Abbreviations and symbols

A	Absorption
A	Acceptor molecule
ALD	Atomic layer deposition
Al_2O_3	Alumina oxide
CPTPP	Carboxyphenyl-triphenyl-porphyrin
CR	Charge recombination
CS	Charge separated state
D	Donor molecule
D-A	Donor Acceptor pair
ET	Electron Transfer
EtOH	Ethanol
G	Glass plate
h	Planck constant, $6{,}62*10^{-34}$ m^2Kg/s
HMDS	Hexamethyldisilazane
HOMO	Highest occupied molecular orbital
InGa	Indium-gallium alloy
ITO	Indium-tin-oxide
LB	Langmuir-Blodgett
LUMO	Lowest unoccupied molecular orbital
LS	Langmuir-Schaeffer
MQ	Milli-Q water
ODA	Octadecylamine
$PDIC_{60}$	Perylene diimide-fullerene dyad
PC_{60}	Porphyrin-fullerene dyad
SAM	Self-Assembly-Monolayer
TiO_2	Titanium dioxide
TR	Transfer ratio
TRMDC	Time-resolved Maxwell displacement charge
ZnO	Zinc oxide
ν	Frequency

1. Introduction

The continuously increasing demand for energy is bringing to a fast and irreversible depletion of the most used natural energy sources such as oil and gas. The expenses related to their extraction and transformations have also made these sources not convenient anymore for a few years. For these reasons the research has already started focusing on alternative energy sources such as wind and marine mills, geothermic energy and solar cells. These last have been recognised among the most promising solutions since their working principle, the photovoltaic effect, is as simple as effective; in addition, provided a careful choice of the building materials a completely *clean* energy can be produced on the contrary to oil and gas sources. Despite this, optimisation of the structure to obtain a satisfactory efficiency is far from being complete.

This work focuses on the preparation and characterisation of model devices for molecular heterojunction organic solar cells. The principal aim is to investigate the photo-induced electron transfer at the interface between the active layer and the semiconductor one. Considerations on the effect of the additional semiconductive layer in the structure are also done. The choice of the materials for the active layer and for the oxide thin film is based on the promising results shown by previous research works [**1**] [**2**]. Porphyrin-fullerene dyads and perylene diimide-fullerene dyads have shown promising absorption properties, with the ability to harvest a rather broad part of the solar spectrum. The study of the photo-induced electron transfer between the two moieties is thus of primary importance in order to understand the dynamic of the response in different illumination conditions and the influence of parameters such as the external applied voltage and resistance variations. The positive effect of an additional layer with accepting properties has been undoubtedly confirmed [**3**] [**2**], yet the ideal material and film morphology are still to be clearly defined. Attempts to use titania and zinc oxide deposited by atomic layer deposition have proven to be successful and are reproduced in this work. Their influence on the photo-voltage response is inspected under variable experimental conditions.

Positive outcomes come from ordered multilayer-based solar cells, therefore different self assembly approaches to deposit thin film were used to produce ordered monolayers. Self Assembled Monolayer (SAM) and Langmuir-Blodgett (LB) methods were used with this work. Moreover a highly ordered monolayer on a likewise ordered oxide film is known to enhance the electron transfer process at the interface between the organic and the oxide layers. The optimisation of the single components of the solar cell, and of the interaction between the different components, would thus lead to an overall increase of the cell performance.

Precise characterisation of the thin film absorbance, via spectroscopic techniques, during the production step is necessary as a quality check. The electron transfer process is studied by means of the time-resolved Maxwell displacement charge technique to analyse the electron movement in the vertical direction only.

2. Theoretical background

The aim of this Thesis was to study the electron transfer at the interface between the organic active layer of donor-acceptor compounds and the semiconductor surface. To understand the possible applications of this kind of devices a brief introduction to the electron transfer mechanism itself and to the photo-activated electron transfer is necessary. The organic photovoltaic cell structure and working principle will be then treated in more detail. To motivate the choice of the used techniques for the deposition of the thin films a description of the self-assembly techniques will be here provided.

The efficiency of the electron transfer mechanism in an organic solar cell depends on several factors such as the active organic compound, the nature of the anode, the temperature and the incident light energy. To analyse the effect of the individual parameters it is necessary to create a simplified model of the solar device for which the variable parameters are the organic active layer and the oxide layer. The studied system can be used to construct a molecular heterojunction organic solar cell.

2.1. Photo-induced Electron Transfer

Electron-Transfer (ET) is a reaction that results in the exchange of a charge between a donor molecule, donor moiety (*D*), and an acceptor one, acceptor moiety (*A*). It can occur when the molecules are either in the ground state or in the excited state. Figure 2.1 schematizes the excited version of this process.
When the excited specie is the donor, D*, an electron is transferred to the acceptor, on the contrary when the excited specie is the acceptor, *A**, a hole will be transferred to the donor.

For the ground state process the driving force for the electron movement is given by the energy difference between the Highest Occupied Molecular Orbital (HOMO) and the Lowest Unoccupied Molecular Orbital (LUMO) levels of the two molecules; the accepting one should have a LUMO level that is lower in energy than the HOMO level of the donating one. A typical example of ground state ET is the charge recombination that follows the photoinduced ET; the electron localized on the acceptor molecule recombines with the hole on the donor molecule leading to the neutrality of the donor-acceptor complex. Generally molecules having electrons in high-energy orbitals, such the ones involved in the π-bond, are feasible of donating an electron; in the same way molecules with unoccupied low-energy orbitals can work well as acceptor [**4**].
For the excited version of the process an additional external source of energy, generally light, is required. In this case the process is defined as *photoinduced* and

at least one of the two moieties should be able of absorbing the light. Only the light activated version of this process will be here analysed being the studied process of this work. In this case the electron transfer process is feasible when the LUMO level of the donor is higher than the LUMO of the acceptor; likewise the hole transfer requires the HOMO level of the donor to be higher than the HOMO of the acceptor. This means that the initial excited level in which the carrier lies must be energetically higher than the final level that the carrier reaches.

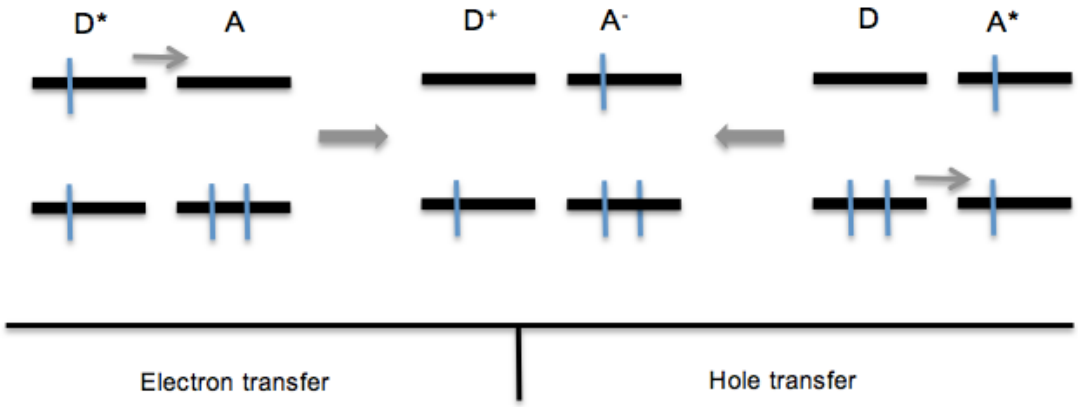

Figure 2.1 *Schematic view of the electron transfer mechanism. The excited specie, either D* or A*, transfers a charge, an electron or a hole respectively, to a ground state nearby molecule, either A or D. This induces the charge localisation on the two molecules: in both cases an electron will be localised on the acceptor moiety and a hole on the donor moiety.*

A competitive process to the electron transfer is the energy transfer. In this case the excited state can be exclusively a donor molecule, and the transfer of energy requires the mutual interaction of electrons belonging to both *D* and *A*. Electron exchange or dipole-dipole interactions are the possible mechanisms through which it occurs [**4**].

The ET process can be described either using a traditional adiabatic reasoning or using a simple yet effective non-adiabatic theory based of Fermi's golden rule. In the former case the reaction steps are described by a motion along a potential energy surface. The reactant moieties are able to gain energy from thermal motions and to form a transition state that corresponds to the maximum associated with the activation energy barrier; the decay into the product state is then a spontaneous process and it is guaranteed once the transition state has been formed. In the latter case the ET rate is highly dependent on the separation distance between the reactants molecules. Fermi's golden rule, indeed, states proportionality between the ET rate and the square of the coupling of the reactant and product electronic states and this last term is proportional to the overlap of the donor and acceptor wavefunctions. The overlap exponentially decreases with the separation distance of the two moieties and is mediated by a coefficient related to the nature of the medium surrounding the molecules. The optimal condition for the ET process to occur corresponds to the maximum overlap and thus to the

condition in which the standard Gibbs free energy gained by the reactants has a similar value to the reorganisation energy, that is the amount of energy required for the distortion of the nuclear geometry of the reactants into the geometry of the products, yet without transfer of the electron. Far from this optimal condition the relationship between the standard Gibbs free energy and the reorganisation energy is a Gaussian one and there is a more strong dependence on the temperature. Basing on the before explained concepts Marcus developed his theory [**5**] according to which the ET process is a single step reaction limited to a short time scale for which the configuration of the nuclei can be considered to be the same for the reactant state and for the product state. The two states are supposed to be weakly coupled and the energy barrier for ET to occur is expressed as the probability of the transfer of one electron. The role of the medium between the molecules is fundamental since it changes its polarisation during the ET thus affecting the ET rate [**6**].

The donor-acceptor distance has proved to be a key parameter since it determines which process will occur: either the desired ET process or any of the unwanted competing processes that usually take place at close separation distances [**7**]. The ET process can also be a sequential one in intramolecular systems enabling the transfer of the electron among many different molecules having fixed distance [**8**]. ET has been observed both in the liquid and in the solid phase. In the former case the moieties need first to approach each other in solution, in the latter a flexible chain or a rigid spacer is required as a connector between the two moieties [**4**]. The basic process is the same in both cases, yet there are some differences due to the higher degree of freedom of the moieties in the liquid state.

2.1.1. Solution electron transfer

Starting from the assumption of neutral *D* and *A* molecules dissolved in solution the electron transfer process can be schematized in the following way [**9**]:

- $D + h\nu \rightarrow D^*$ photo-excitation of D
- $D^* + A \rightarrow (D\text{-}A)^*$ exciplex formation
- $(D\text{-}A)^* \rightarrow (D^{\delta+}\text{-}A^{\delta-})^*$ polarisation of the excitation
- $(D^{\delta+}\text{-}A^{\delta-})^* \rightarrow (D^{\bullet+}\text{-}A^{\bullet-})$ ion-radical pair formation
- $(D^{\bullet+}\text{-}A^{\bullet-}) \rightarrow D^{\bullet+} + A^{\bullet-}$ moieties separation
- $D^{\bullet+} + A^{\bullet-} \rightarrow D + A$ charge recombination

The absorption of a photon by the donor molecule induces its photo-excitation to *D**. If an acceptor molecule, *A*, is at a distance close enough to interact with *D** the ET can occur; *D** and *A* can either form a complex called exciplex, intramolecular ET, or interact with each other without forming any common excited state, intermolecular ET. In the first case the exciplex formation induces the

delocalisation of the excitation over the whole compound first and subsequently the polarisation of the moieties. This last step localizes the positive charge on the donor moiety and the negative one on the acceptor moiety. An ion pair is then formed inside the complex and lately the two molecules are divided forming a solvent separated ion pair. These charges can finally recombine to give the starting molecules, charge recombination process (CR), or can be used for other reactions.
In case no exciplex is formed the reaction steps require the direct passage from the excited donor molecule, D^*, to the localisation of the charges on the acceptor and on the donor, forming thus A^- and D^+. The described steps refer to an intramolecular ET in a liquid phase for which the involved species have a high degree of freedom and thus they can move and rearrange in different ways [**9**]. Depending on viscosity the solvent is able to change its polarisation to stabilize the excess of negative and positive charges on the two moieties [**6**].

2.1.2. Solid state electron transfer

The solid state ET process mainly differentiates from the one in solution because *D* and *A* are covalently linked and the reaction steps are more straightforward. In this case the photo excitation of *D* coincides with the formation of the exciplex and the charge separation occurs directly from this step as presented below:

- $D \mid A + h\nu \rightarrow D^* \mid A$ donor photo-excitation
- $D^* \mid A \rightarrow D^+ \mid A^-$ charge separation

Since the two moieties are covalently linked there is a higher probability of charge recombination of $D^+|A^-$ to $D|A$ complex as compared to the liquid phase one; on the other hand the closer the two moieties are, the more efficient the charge separation process is. To slow down this process and avoid unwanted recombination secondary levels of donor and acceptor moieties can be used. These can be either organic species similar to *D* and *A* or metallic molecules. The relative orientation of the molecules affects the efficiency of the process and its duration. Depending on the path the transferred electron is moving into going from *D* to *A*, the process can favour the recombination on different degrees and it can take place in a relatively short or long time [**9**] [**6**].

2.2. Solar cells

Any device capable of transforming the solar energy, namely light, into electric energy can be defined as a solar cell. Since this effect has been observed for the first time by Becquerel in 1839, lot of research has been done so that nowadays three categories, or generations, of solar cell devices can be identified. They differ

in many ways going from their working principle and the portion of the solar spectrum absorbed, to the materials they are made of and their efficiency.

2.2.1. The three generations

The first generation is based on the silicon technology and on p-n junction. For mono-crystalline silicon layers efficiency up to 25% were obtained in laboratory [**10**]. The demand for lighter, less expensive and more recyclable devices favoured the development of the second generation of solar cells. These are based on the thin films technology and include amorphous silicon cells, cadmium-telluride cells and the so called CIS and CIGS cells, based on copper-indium-gallium selenide. The most efficient thin film solar cells are though the ones based on compounds of III and IV group elements; multiple junctions devices based on these materials gave up to 40% laboratory efficiencies. Both the high cost and the toxicity of some of the components limited the use of these cells [**10**].
The third generation category is broader than the previous two and includes both organic and inorganic materials as well as cells based on the p-n junction and on different mechanisms. Tandem cells, intermediate band cells, organic cells, dye-sensitized cells are just a few examples. Among these types of solar cells particular interest arose for the organic cells, which tend to mimic the natural process of photosynthesis for the utilization of light [**11**] [**12**]
A possible classification for the organic solar cells is based on the nature of the photoactive components. The following types of cells can thus be identified:

- Dye / dye
- Dye /TiO_2 (Graetzel cells)
- Polymer / dye
- Polymer / polymer
- Polymer / fullerene
- Polymer / inorganic
- Polymer / quantum-dots

The first specie accounts for the donor, whereas the second one for the acceptor. Since in this work the dye played both the role of the donor and of the acceptor the focus will be on that type of cell, that can be defined as an heterojunction organic solar cell, leaving the literature [**13**] [**14**] for further readings about the other possible types of cells.

2.2.2. Organic solar cell structure

The components of an heterojunction organic solar cell, whose schematic structure is presented in Figure 2.2, are the ones typical for every photovoltaic device; namely a material able to absorb photons and generate the charges, electron and holes, and two electrodes, one of which must be transparent, to allow the light to get to the photoactive part. Common materials are Indium Tin Oxide (**ITO**) for the transparent electrode and aluminium for the other electrode. The active material can either be a semiconductor or an organic dye molecule. In this last case the higher is the conjugation of the molecule the lower will be the gap between HOMO and LUMO and thus the larger the fraction of the visible spectrum that is absorbed. Condensed polycyclic hydrocarbons as pentene, organic dyes as phtalocyanines and conjugated polymers as polyacetylene or polythiophene satisfy the previous conditions [**13**] [**15**]. It has been found that the most efficient devices are the ones for which the active layer is made by one thin film of organic molecules with the absorbing function, the donor layer, and by another layer made by molecules with the accepting function, the acceptor layer.

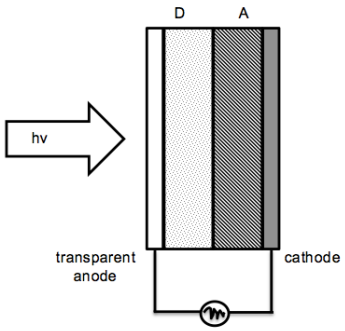

Figure 2.2 *Schematic structure of an organic solar cell. The donor, D, and acceptor, A, layers are sandwiched between the cathode and the transparent anode. The light will impinge on the cell from the transparent anode side.*

The choice of the active layer material and of the electrode material should be done taking into account the relative work-functions so that the electron and hole transfer is possible and the efficiency reaches the highest value. De-excitation and recombination processes should be avoided as well.

D and A films can either be made of monolayer or multilayers structure. In the former case a high efficiency crystalline structure is formed; in the latter case a more disordered and amorphous molecular distribution occurs. The monolayer configuration ensures a quite low absorption not allowing the complete harvesting of the solar spectrum. On the contrary the high degree of order of the molecules in the monolayer warrants a directional movement of the electrons; the probability of lateral interactions, and thus of inefficient charge recombination in the active layer, is thus minimized. The multilayer structure would assure a higher harvesting of the solar spectrum, yet the directional movement of the electrons

would be less efficient. A promising solution is the bulk-heterojunction in which the D and A moieties form a nanoblend, with extension of the domains comparable to the diffusion length of the exciton, few nanometres, This structure guarantees at the same time a directional movement of the electrons and a higher absorption of the light [**15**] [**16**].

2.2.3. Working principle

Upon illumination of the organic solar cell the donor molecule absorbs a photon and promotes one of its electrons from the HOMO level to the LUMO level, forming thus an excited complex called exciton. Two alternative processes can occur now: either the exciton recombines with the hole left in donor molecule yielding to luminescence, unwanted process, or the exciton can give that electron to another material, desired process.

The electron extraction from the excited complex is carried out by another material provided that it is in contact with the donor molecule and it has different electronics properties from it. This role is played by the acceptor molecule, which dissociates the exciton into two separated charges, an electron and a hole; they are localized on the acceptor and donor molecules, respectively. Without the presence of an acceptor material the charge separation can be performed by the junction between the organic layer and the cathode, yet with a lower efficiency [**13**] [**15**].

The electron is then transferred from the LUMO level of the acceptor material towards the cathode whereas the hole from the HOMO level of the donor towards the anode. If a load is applied a current flow is thus produced [**14**]. Figure 2.3 graphically explains this mechanism.

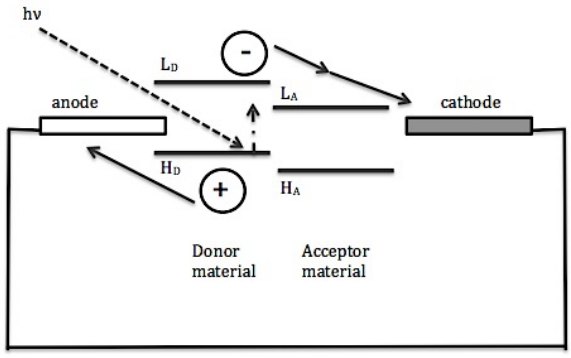

Figure 2.3 *Graphic representation of the working principle of an organic solar cell. The absorption of a photon induces the promotion of an electron from the HOMO level to the LUMO level of the donor molecule, originating an exciton. The acceptor material breaks the exciton into a positive charge and a negative one. The carrier gradient induces the electron movement towards the cathode and the hole movement towards the anode.*

The electron and holes movement towards the electrodes is supported by the built-in electric field that is the carrier gradient existing between the electrodes-

organic layer interface and the bulk of the electrodes. After the charge separation holes and electrons accumulate at the surface of the electrodes, yet few of them can be found in the bulk.
The efficiency of the cell is maximized once the interfacial surface area between the donor and the acceptor layer is maximized. In this way every exciton that is generated by the donor will find an interface, the acceptor molecule, able to create the electron–hole pair.

2.3. Active layer components

The role of the dye in an organic solar cell is to harvest the light and create a charge separated state so that the electron and hole injections in the oxide layer can occur.
Phtalocyanine and porphyrins are among the most used dyes nowadays. Promising possibilities are shown by supramolecular compounds in which the donor and acceptor roles are performed by two different moieties.
The choice of the active component determines the absorbed portion of the solar spectrum; minor differences in the chosen functional group and in the position of its attachment to the main molecule will affect the absorption range. The molecular organization of the single molecules also affects the absorption properties.
The donor and acceptor moieties used in this work are treated first individually and then together, as dyads enhancing their photochemical properties.

2.3.1. Electron-donor and electron-acceptor materials

Porphyrin molecules are natural occurring hydrophobic macrocycles made by four pyrrole rings linked by methane bridges; their basic structure is the porphine and it is presented in Figure 2.5. They can be functionalized by addition of metallic atoms in the π-core ring to form 1:1 complexes or by the presence of peripheral functional groups; in this case they are defined as *metallized* porphyrins, otherwise as *free-base* porphyrins.
The macrocycle itself is planar yet the presence of specific functional groups can lead to non-planarity, to a different steric hindrance and to the conformational distortion of the π-core. This functionalization modifies the photochemical and the electrochemical properties. For instance, when the central ring accepts two protons a bond between the two inner nitrogen atoms is formed and localisation of two positive charges in the central part of the macrocycle occurs. The induced change in absorption can be seen as a change in the colour of the porphyrin based solution from red to green [**17**].

Absorption spectrum of a free-base porphyrin presents five typical bands in the visible region: the high intensity Soret band at 420 nm and the lower intensity Q bands at longer wavelength as depicted in Figure 2.4 [**18**]. Change in absorption

spectrum due to interactions with the environment makes them very precise sensors. For particular porphyrin derivatives, such as the tetrakis-methyl-pyridinium porphyrin, an increase in the polarity of the solvent they are dissolved into leads to a blue shift of the Soret band. The protonation of the π-core of those porphyrins causes, instead, the disappearance of two of the Q-bands. [**19**]

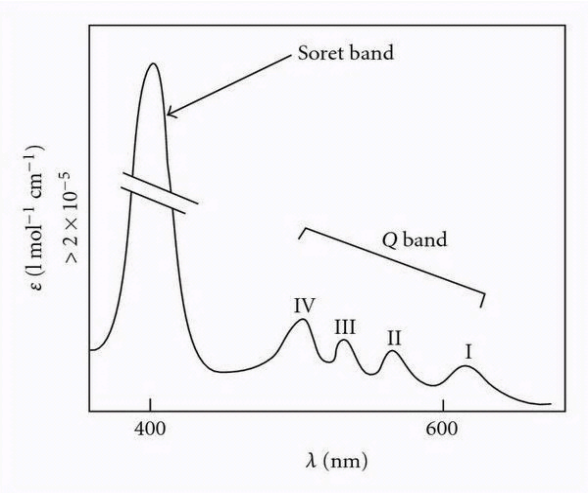

Figure 2.4 *Typical features of a porphine absorption spectrum. The high intensity Soret band is visible around 400 nm and the lower intensity Q bands at longer wavelengths.* **[**20**]**

The presence of the π-core makes this class of molecules highly efficiently in electron transfer processes; in particular they can work as electron donors. Moreover the absence of relevant structural changes as a consequence of the electron transfer and the small reorganization energy make them very stable and suitable for a large variety of applications [**21**] [**22**].

Perylen-diimides are a class of molecules made by a perylene backbone to which imide groups are attached in peri position. According to the number, n, of naphthalene groups present in the backbone a homologous series of aromatic compounds is formed: going from perylene diimide (PDI), n=0, to terrylene (TDI), n=1 and quaterrylenebis(dicarboxyimide) (QDI), n=2.
They are well known for their strong coloration going form dark green to red, violet and black. Their properties can be tailored changing the number of imide groups and the substituents linked to each of them, the simplest structure is shown in Figure 2.5. Both the nature of the substituents and the position they are attached to, *peri* on the top or *bay* on the sides, determine the resulting optical properties.
For example the addition of naphthalene groups along the backbone leads to a red shift of 100 nm of the absorption bands for each added group. For PDI the peak is at 580 nm, whereas for QDI it is around 780 nm [**23**].

PDI molecules exhibit excellent chemical and photochemical stability and strong absorption in the visible and near infrared part of the solar spectrum. Due to their significant charge transport properties they find applications as sensors and in dye sensitized solar cells both as electron acceptor and electron donor molecules. The role played in the electron transfer process depends on the specific functionalization of the perylene derivative; in particular the *bay* functionalization leads to good electron donating properties [**24**].

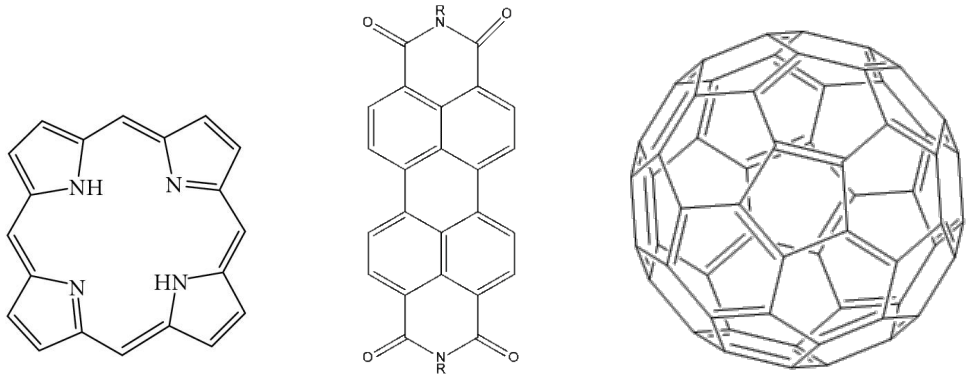

porphine perylene diimide fullerene

Figure 2.5 *Chemical structure of porphine, perylene diimide and fullerene C_{60}.*

As depicted in Figure 2.5 fullerenes are hollow cage structures entirely made by carbon atoms, with sp^2 hybridization, arranged in hexagonal and pentagonal configurations. The number, n, of carbon atoms can vary from 20 to 100; among the possible configurations C_{60} and C_{70} are the most used ones owing to the high stability given by the truncated icosahedron structure.
Due to their small reorganization energies and the minimal changes associated with the electron transfer reaction they are used as electron acceptor molecules [**25**]. C_{60} in particular is able to accept up to 6 electrons getting thus easily reduced; its oxidation is also possible though it is more difficult. Fullerenes absorption spectrum is characterized by intense absorbance in the UV region and by a weaker one in the visible region. Fullerene derivatives are nowadays studied to form highly functionalised supramolecular structures [**9**].

2.3.2. Donor-Acceptor dyads

A supramolecular structure made by an electron-donor moiety and by an electron-acceptor one enhances the harvesting photovoltaic properties of the single acceptor and donating molecules. The two moieties are covalently linked so that dyad, triad, tetrad or pentad structures are formed. When there is more than one acceptor moiety several accepting levels are formed thus prolonging the lifetime of the charge separated state. The connection between donor and acceptor moieties is also done so that a directional electron transfer occurs [**25**].

Porphyrin-fullerene dyads in solution are known to exhibit excellent ET properties due to their small reorganization energy. Upon illumination a fast charge separation occurs followed by a slow charge recombination. The charge-separated state is thus a long-lived one with a high quantum yield. Referring to the Marcus theory [**5**] this means that the electron transfer from the excited porphyrin to the fullerene occurs close to the top area of the parabolic curve whereas the charge recombination occurs in the inverted region of the Marcus parabolic curve.
The ET behaviour of porphyrin-fullerene dyads in molecular assemblies, like in thin films for instance, is a widely studied subject. ET is affected both by the interactions with the surroundings molecules and with the environment and by the orientation of the dyad molecules [**26**].

PDI-fullerene dyads are another efficient example of donor acceptor couple in which the perylene derivative has the donor role whereas the fullerene works as an acceptor molecule. The longest lifetimes were observed for compounds in which the fullerene was attached to the bay position of the perylene diimide rather than to the peri position [**24**].

2.4. Oxide Role

The presence of a buffer semiconductor layer between the cathode and the active layer of an organic solar cell is believed to have a strong influence on the cell behaviour. This additional oxide layer is capable of accepting the electrons coming from the charged acceptor organic moieties, A^-, thus creating a secondary electron transfer process, and to transfer them to the cathode due to their semiconductive properties. The thickness of the film has to be wisely tuned to minimize the presence of defects and electron traps that would delay the electrons movement. Depending on the chosen material it is also possible to tune the band gap of the cell and thus the harvested portion of the solar spectrum. The choice of the oxide is thus ruled by its energy gap and by the nature of the dyad it is in contact with; a stable and strong bond should be formed with the dyad and the conduction band of the oxide should be lower than the LUMO level of the acceptor moiety. Zinc oxide and titanium dioxide are known to covalently bond with fullerenes and porphyrins, via carboxyl and triethoxysilane anchoring group, and to have electron accepting properties towards them. Nanostructured oxide thin films [**2**] and porous films have been reported to enhance the overall performance of the solar cell in the described way [**3**].

2.5. Sample manufacturing processes

In order to observe the vectorial electron transfer in a thin film the molecules must have homogeneous organisation all over the film so that the electron movement will be the consistent through the film. This section presents two of the most important thin film deposition techniques [**27**] [**28**] that are capable of forming such organized structures, namely Self Assembling Monolayer (SAM) and Langmuir-Blodgett (LB). For both methods the driving force for the monolayer formation is given by the auto organisation of the building blocks of the film.

2.5.1. Self-Assembling-Monolayer deposition

Self-Assembly is a term that refers to the spontaneous organization of randomly distributed objects into a precise pattern due to local interactions. This molecular rearrangement leads to a more stable state and preserves the nature of the single building blocks. These can be atoms, single molecules or supramolecular structures.
Since the individual nature of each building block has not to be altered no covalent bonds are formed among them; rather electrostatic, dispersive or hydrogen bonds and coordination interactions will occur [**29**]. The size and shape of the final structure can be adequately tailored; nowadays the most versatile and studied self-assembly technique is the one aimed to the production of monolayers, SAM [**27**]. This self-assembly can be exploited both for organic and metallic ligands. The organisation can take place at a solid–liquid interface or at a liquid-gas (generally vacuum) one; in both cases the monolayer will form on the surface of the densest phase.

The nature of the formed pattern depends mainly on the balance between the molecule-molecule interactions and the molecule-substrate ones. The former is mostly determined by the specific functional groups of the assembling molecules; the latter by the possible presence of specific high-energy adsorption sites and by the homogeneity of the surface for example. Generally the molecules will arrange in a geometry that will lead to the minimum energy of the system. The structure of the assembling molecules influences the geometry of the formed film: planar molecules with bulky peripheral substituents will try to maximize the covered area on the substrate thus arranging parallel to it; molecules with heteroatoms will try to maximize the overlap of the heteroatoms lone pairs; the orientation of the molecule with respect to the surface can be fixed once the molecule possesses two or more heteroatoms.

For the particular case of a film forming at a liquid-solid interface this method requires the dissolution of the desired compound into a solvent and the immersion of the substrate in the so obtained solution.

The molecules start to organize on the solid support and in a relatively short time an almost complete film is formed; if the support is kept in the solution for longer times the reorganization of the molecules will take place so that a defect free film is formed.
The immersion time depends on the specific compound used and on the nature and morphology of the support. It can be experimentally determined by means of absorption measurements. The minimum immersion time after which no changes in the absorption spectrum can be detected can be considered as the time necessary to completely assemble a layer on the substrate surface.
The so obtained structure needs to be properly rinsed at the end of the process to remove any exceeding molecules that may have been physically absorbed. The rinsing medium is typically the solvent the solution was prepared with.
The obtained film presents molecules uniformly oriented and organized on the support surface. If proper immersion times are used and the interactions between the deposited molecules and the support are strong, only minor defects are present on the film.

Among the most outstanding applications of SAM there are chemical sensors and biosensors. Changes in the electrical conductivity or in the mechanical properties of the samples reveal the interaction with a specific molecule in that environment [**30**]. Due to the high organization degree of the molecules the SAM technique is used for application in which a directional electron movement is required, such as in solar cell active layers.
When the monolayer formation is supported by an external aid, mechanical barrier or applied voltage, this technique is referred to with the name of the particular device or the scientist who discovered it. The Langmuir-Blodgett deposition and electrochemical cell deposition are two possible examples.

2.5.2. Langmuir-Blodgett deposition

The Langmuir-Blodgett technique is a particular type of SAM for which the film formation on the solid substrate consists of two separately steps. First a floating film has to be formed on the surface of a buffer solution and only after that it can be transferred onto a solid support. As in the previously described SAM the nature of the building blocks is preserved during the formation of the film. A broad variety of molecules can be used for this technique provided they are amphiphilic, that is they contain two functional groups with different polarity properties; one of them should be hydrophilic and the other hydrophobic.

The floating film formation is briefly schematized in Figure 2.6. A solution of the chosen molecules is spread on a liquid surface, the buffer layer. Attention must be paid so that the molecules are insoluble in the buffer layer but can anchor to its surface and that the solvent evaporates at the working temperature and pressure

conditions. After solvent evaporation only the molecules that will be the building blocks will remain on the surface. Those molecules are then progressively compressed by means of two mechanical barriers till a compact film is formed.

During this process the molecules experience three different phases with variable organization degree. At the beginning they are in the gas state, being the interactions between the molecules negligible and the organization degree almost null. During the compression step the interactions among the molecules increase and a short-range organization can be observed leading to the formation of a less loosely two dimensional packed structure; this can be described as the liquid expanded phase. At the end of the compression the molecules are organized in what can be ascribed as the condensed solid phase. The orientation of the molecules is homogeneous over the whole film surface and it is ruled by the molecules-buffer layer interactions. At this point the floating solid film can be transferred onto an external substrate.

The phase changes are monitored during the film formation via the pressure-area isotherm. An example of this plot is presented in Figure 2.6 and it expresses the change of the surface pressure of the molecules spread on the film as a function of the mean molecular area, the area occupied by each molecule in the different phases. The general trend requires an increase in the surface pressure as the surface area decreases due to the increased interactions among the molecules. When the molecules are in the gas state the surface pressure has its minimum values and the mean molecular area the maximum one; as the compression progresses the surface pressure increases gradually and conversely the occupied area per molecule decreases reaching the limit value when the solid state is achieved.

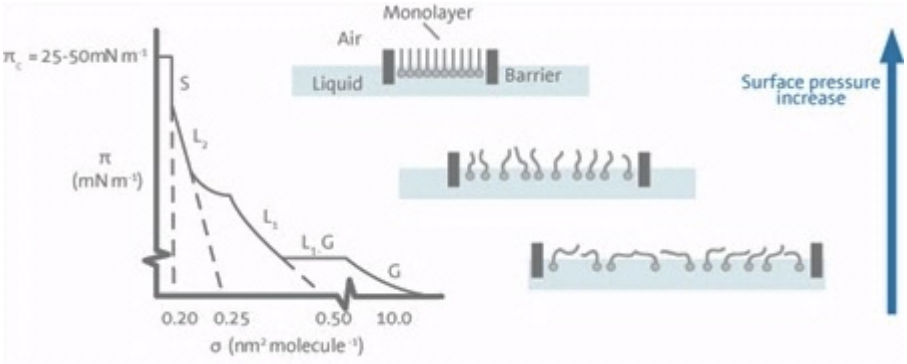

Figure 2.6 *Floating film formation and corresponding isotherm. As the molecules compression progresses a more ordered structure is formed. The molecules occupy lower areas and the associated pressure increases. Transitions from the gas to the expanded liquid and condensed solid state occur as the monolayer is compressed.* [31]

The pressure increase rate changes from phase to phase and it's highly dependent on the nature of the used molecules. Each kink in the graph corresponds to a phase change; phase coexistency is expressed by a decrease in the area at constant pressure values. Changes in the buffer solution do not affect the shape of the isotherm curve. Further compression of the monolayer after reaching the solid state leads to the collapse of the film on itself; a three dimensional structure is formed and pressure fluctuations are observed. It is thus fundamental to know the limiting pressure value, target value, for which an ordered monolayer is formed thus avoiding the subsequent ruin of the film [**32**] [**33**].

The film transfer can be performed in two different ways as presented in Figure 2.7. The Langmuir-Blodgett technique requires the lifting of a solid plate perpendicularly to the floating film. The monolayer will be transferred on both sides of the plate. Lifting the plate in the downward direction or in the upward will determine the orientation of the molecules on the film. In case of an upward lifting the plate has to be immersed in the buffer solution prior to the floating film formation.

To obtain multilayer structures the plate can be re-immersed in the same solution several times. As the number of layers increases the fragility of the structure increases as well. A progressive decrease in the internal organisation of the film is also expected. According to the orientation of the molecules on the film three types of deposition can be distinguished: X-type, Y-type and Z-type. The X-type refers to a film for which the hydrophobic tails of the molecules anchor on the support and the Z-type counts for the opposite situation. Y-type refers to a multilayer structure in which there is an alternation of the molecules orientation from one layer to the next one [**34**].

The other film transfer possibility is called Langmuir-Schaeffer (LS) and it requires the plate approaching parallel to the floating film. In this case the film is formed on one side only of the plate. Constant target pressure is necessary to assure the homogeneous transfer of the film.

The quality of the film is controlled via the Transfer Ratio (TR) that is the ratio between the area of the molecules removed from the floating monolayer after the film transfer and the support area. It ranges between zero and one; values in the 0,9-1,05 range are indicative of a successful transfer and thus of a homogenous film [**35**].

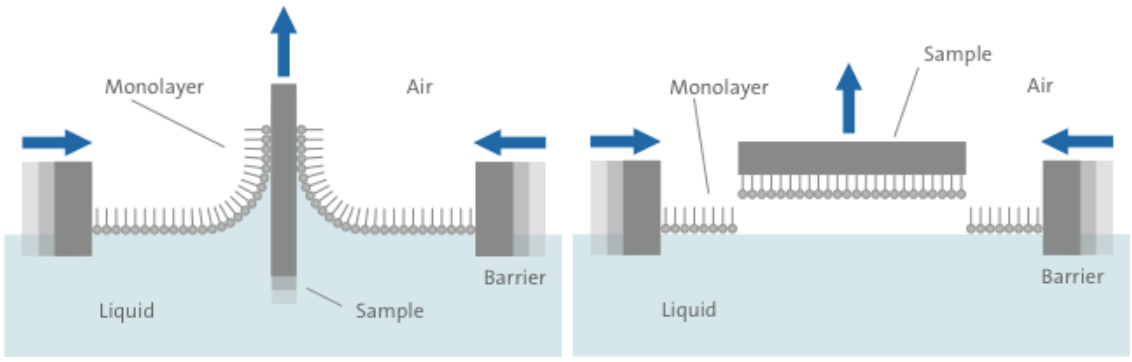

Figure 2.7 *Monolayer transfer onto a solid substrate via LB, on the left, and LS technique, on the right. The monolayer is formed on both sides of the plate in the former case and on one side only in the latter. Molecular orientation can be tailored through the dipping direction for the LB technique* [31].

This technique permits the formation of films with a very precise control in thickness, molecular orientation and packaging density over a few square centimetres area. The thickness will depend on the size of the molecules; if a non-symmetric molecule is used, the interactions between the functional groups of the molecule and the buffer layer and the solid substrate determine the relative orientation of the molecules and thus the final film thickness.

It is thus fundamental to use amphiphilic molecules to control this type of interactions. If a water based buffer solution is used the hydrophilic group of the amphiphilic molecule will be immersed in the solution and the hydrophobic one will be exposed to air. To deposit this specific molecule on a hydrophilic substrate lifting from solution to air will be necessary. Vice versa to deposit it on a hydrophobic one the lifting direction will be the opposite one. Non amphiphilic molecules can be used only on the condition that they are mixed with amphiphilic ones. More amorphous films with thicknesses over one monolayer are obtained in this case. Inhomogeneities in the molecules packing, impurity and voids can be present even if great precautions were taken during the film formation [**36**] [**32**]. Possible applications of these films are functional coatings with tailored optical and structural properties, novel coatings made by nanotubes [**37**] or nanorods [**38**] for instance, and biosensor [**39**].

3. Materials and methods

In this chapter the principal compounds used for this work are listed and briefly presented. The sample manufacturing and study methods, as well as data analysis routines are explained. The samples are divided into two different sets according to the aim they were prepared for. The first set refers to simple monolayer and bilayer structures used for the characterisation of the organic compounds; the second one was properly manufactured to be used for photo-voltage measurements.

3.1. Materials

The D-A pairs used in this Thesis were synthesized at the Department of Chemistry and Bioengineering, Tampere University of Technology. The free-base porphyrin was purchased from Sigma Aldrich. Figure 3.1 presents the molecular structure of these compounds: from left to right carboxyphenyl-triphenyl-porphyrin (**CPTPP**), porphyrin-fullerene dyad (**PC_{60}**), and perylene diimide-fullerene dyad (**$PDIC_{60}$**).
Fullerene C_{60} was used as electron accepting moiety in the dyads whereas perylene diimide, PDI, and porphyrin, P, were used as electron donating moieties in **$PDIC_{60}$** and **PC_{60}** dyads. In the **$PDIC_{60}$** the two moieties are connected by a single linker whereas in **PC_{60}** by two linkers.

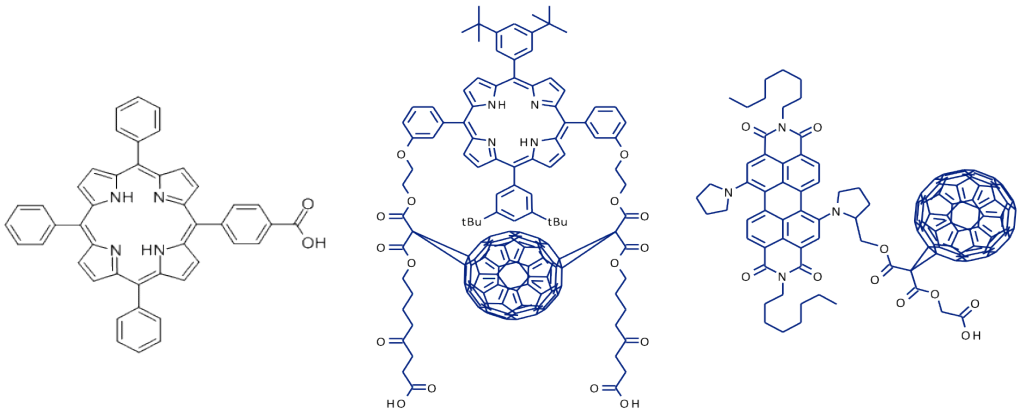

CPTPP PC_{60} $PDIC_{60}$

Figure 3.1 *Chemical structures of the used compounds. From left to right CPTPP, PC_{60} and $PDIC_{60}$.*

Thin films of **Al_2O_3**, **TiO_2** and **ZnO** were deposited at Aalto University by atomic layer deposition method. All the other compounds were commercially available and they were used without further purification.
Ethanol and chloroform were chosen as solvents for the study of the afore mentioned compounds in solution. Zinc-acetate was the precursor for the zinc

oxide layers obtained via spin coating. De-ionized Milli-Q water (MQ) and a 0,6 mM phosphate buffer solution were used as sub-phase for LB and LS film depositions. Hexamethyldisilazane (HMDS) was used for the hydrophobic treatment of the photo-voltage samples, and octadecylamine (ODA) was used to deposit external insulating layers.
From now on the samples will be referred to using the name of the substrate and of the organic compound deposited on it. Additional elements common to a whole set of samples will be omitted after proper declaration.

3.2. Deposition techniques

The deposition techniques used for this work are briefly reviewed in this section. The used experimental settings and parameters are listed.

3.2.1. Self-Assembly-Monolayer deposition

SAM depositions via dipping of the solid support into a solution of photoactive compounds with surface active groups were carried out to prepare both samples for absorption and for photo-voltage measurements.
To favour the molecules chemical adsorption the plates, either **ITO|ZnO** or **G|ZnO**, were heated up to 150°C for approximately 30 minutes.
CPTTP monolayers on **ITO|ZnO** and **G|ZnO** were obtained by immersing the substrates in a 0,15 mM solution in EtOH for 30 minutes. To form a **PC_{60}** monolayer on **G|ZnO** the plate was immersed for 40 minutes in a 0,81mM **PC_{60}** EtOH:$CHCl_3$ (2:1) solution. For **$PDIC_{60}$** a 0,36 mM solution in EtOH:$CHCl_3$ (2:1) was used with 60 minutes as immersion time.
For the photo-voltage samples the same dyad solutions were used yet increasing the immersion times. To obtain **PC_{60}** films on **TiO_2**, **Al_2O_3** and **ZnO** the immersion time was 3 hours whereas to obtain a **$PDIC_{60}$** film on the same type of substrates 16-19 hours immersion were necessary.
At the end of the immersion the plates were carefully rinsed, with the solvents used for SAM deposition, to remove any physically adsorbed molecules.

3.2.2. Langmuir-Blodgett deposition

In this study both a KSV Single and a KSV Mini LB troughs [**31**], were used to record the isotherm of each compound and to deposit single and multiple monolayers.

The surface pressure-mean molecular area isotherms for each compound were recorded using MQ water as sub-phase and barrier velocity of 1 mm/min. Free-porphyrin and dyad monolayers were deposited on glass substrates by moving the substrates in the direction from solution to air with a lifting velocity of

10 mm/min. The target pressures for film depositions were determined from the isotherm curves.
ODA films were deposited on the samples prepared for the photo-voltage measurement using the Single trough instrument. A 0,6 mM phosphate buffer solution was used as buffer sub-phase and a 3,71 mM ODA (4 mg/ml) solution in chloroform to form the ODA floating monolayer. The estimated target pressure for the formation of an ODA film was 22 mN/m. The first layer was deposited immersing the plate in the solution with a downward velocity of 40 mm/s; the subsequent downward and upward immersions were carried out at 20 mm/s. Before each re-immersion the plate was left to dry under the trough for 600 s.

3.2.3. Spin-coating

The spin-coating method is a straightforward thin film deposition technique commonly used for its simplicity and short preparation times. An exceeding amount of the precursor compound is poured onto the substrate surface; this one is then rotated at high velocity in nitrogen atmosphere in order to uniformly spread the solution on the surface and evaporate the solvent. The thickness of the film can be controlled by tuning the rotation velocity and the volume of precursor used.

For this study the WS-400B-6NPP/LITE spin coater [**40**] was used to obtain **ZnO** precursor films on glass substrates using a zinc-acetate solution (50mg/ml in 96%-methoxy ethanol and 4% ethanolamine) with 1 minute as target time and 2000 round per minute. After spin coating the samples were annealed at 350 °C for 20 minutes to convert zinc-acetate layer to zinc-oxide film.

3.3. Samples preparation

As already mentioned two different sets of samples were prepared during this work: one for absorption measurements and compound characterisation and one for photo-voltage tests. The step-by-step procedure to manufacture both sets of sample is briefly described here.

3.3.1. Samples for spectroscopy studies

Standard laboratory glass plates and **ITO** plates were cleaned following an ordinary procedure [**33**]. A few plates were coated with a zinc-oxide layer via spin coating technique and then annealed to obtain the semiconductor film.
The deposition of the organic monolayers was then carried out using the LB, LS and SAM techniques with properly concentrated solutions of **CPTPP**, **PIC_{60}** and **$PDIC_{60}$**. First the monolayers were deposited on glass plates via LB. When

successful results, in terms of transfer ratio and absorption intensity, were obtained depositions of the same compounds on **G|ZnO** were carried out.
Finally SAM depositions on **ITO|ZnO** substrates were carried out for all organic compounds. The so obtained samples were stored in glass containers and analysed with a spectrophotometer without further cleaning.

3.3.2. Samples for photo-voltage measurements

The assembling of the photo-voltage samples was carried in collaboration with Aalto University, Helsinki. Glass substrates coated with **ITO** (sheet resistance 8 Ω/sq) as transparent conductive oxide were preliminarily cleaned in ultrasonic bath in acetone, chloroform, sodium dodecyl sulphate (40 mg/l), distilled water and 2-propanol. The plates were then dried in vacuum at 150°C for 1 hour.
Aalto University performed the ALD deposition of the oxide monolayers, using a Beneq TFS-500 reactor at the working temperature of 200°C. The film precursors were trimethylaluminum and water, titanium tetrachloride and water, diethylzinc and water for the $\mathbf{Al_2O_3}$, $\mathbf{TiO_2}$ and **ZnO** films, respectively. Three sets of samples were thus obtained: **ITO|**$\mathbf{Al_2O_3}$, **ITO|**$\mathbf{Al_2O_3}$**|**$\mathbf{TiO_2}$ and **ITO|**$\mathbf{Al_2O_3}$**|ZnO**.

The subsequent treatments were carried out at Tampere University of Technology. SAMs of $\mathbf{PC_{60}}$ and $\mathbf{PDIC_{60}}$ were deposited by immersing the plates in 0,81 mM $\mathbf{PC_{60}}$ and 0,36 mM $\mathbf{PDIC_{60}}$ solutions, respectively. The SAM deposition of $\mathbf{PC_{60}}$ proved to be successful for all the substrates, whereas $\mathbf{PDIC_{60}}$ was only deposited on **ZnO** substrate. **ITO|**$\mathbf{Al_2O_3}$ and **ITO|**$\mathbf{Al_2O_3}$**|**$\mathbf{TiO_2}$ with $\mathbf{PDIC_{60}}$ could thus not be prepared for photo-voltage measurements. After the deposition the of donor-acceptor layer the plates were immersed in a HMDS solution in equilibrium with its vapour phase for 10-15 hours at room temperature to increase the hydrophobicity of the surface and thus to improve the quality of the subsequent deposition of LB insulating layers. The LB deposition of 20 ODA layers was then carried out using a phosphate buffer solution.
The obtained devices were then stored in glass containers. Spectroscopic measurements were carried out on all the plates without further cleaning. Photo-voltage measurements were carried out on four sets only, **ITO|**$\mathbf{Al_2O_3}$**|**$\mathbf{PC_{60}}$, **ITO|**$\mathbf{Al_2O_3}$**|**$\mathbf{TiO_2}$**|**$\mathbf{PC_{60}}$, **ITO|**$\mathbf{Al_2O_3}$**|ZnO|**$\mathbf{PC_{60}}$ and **ITO|**$\mathbf{Al_2O_3}$**|ZnO|**$\mathbf{PDIC_{60}}$, for the already said reasons. From now on these samples will be referred to specifying the name of the organic layer and of the closest underneath oxide layer only. A schematic presentation of the samples is shown in Figure 3.2.

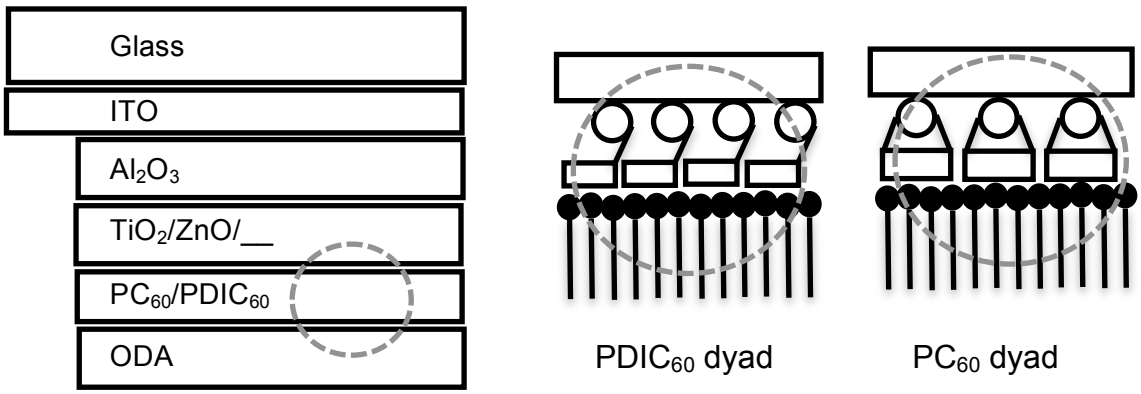

Figure 3.2 *Schematic view of the photo-voltage samples and relative orientation of the molecules in the active layer. The fullerene moiety is represented by the circle, the porphyrin and the perylene diimide ones by the rectangle and the ODA molecules by the sticks, respectively.*

Reference samples, without organic layer, were necessary for the photo-voltage measurements. They were manufactured in a similar way to the real samples but without dyad layer, which means that the ALD deposition of either alumina, titania or zinc oxide was directly followed by HMDS treatment and LB deposition of 20 ODA layers.

3.4. Thin film characterization

The quality of the LB films prepared in this study was characterized by the transfer ratio value where TR equal to one was indicative of a good film and TR equal to zero of a not formed film.
Spectroscopic and photoelectrical methods were then used to characterize all the prepared films. The former provided information regarding the absorption characteristics of the used compounds and the quantity of molecules in the films, whereas the latter offered data relative to the electron transfer in the active layer and at the semiconductor-active layer interface. To analyse the obtained results the programs Decfit and Origin 8 were used. In this section the experimental methods are briefly explained.

3.4.1. Spectroscopic method

Steady state absorption measurements were carried out using a UV-3600 Shimadzu spectrophotometer, in the 300-850 nm range with 0,1 nm resolution. For solution measurements one pair of matching glass cuvettes, optical path length l=1 cm, was used. For thin films deposited directly on glass or on a **ZnO** layer, another glass plate, or a plate with a pristine **ZnO** layer, were used as a reference. For complex structures, made of several and different films, a mathematical

manipulation allowed the determination of the signal corresponding to a precise layer only, generally the outmost one.
Suppose absorption of a substrate before deposition of organic layer, e.g. monolayer of dyad molecules, is A(λ), and after the deposition it is B(λ), then the absorption of the organic layer only C(λ) = B(λ) – A(λ). In other words, the absorption of the sample before deposition of the photoactive layer is used as a reference spectrum, which is subtracted from the spectrum of the sample with photoactive layer.
Absorption spectra were used to monitor the used solutions and to regularly check the quality of the manufactured thin films monitoring the change in absorbance of the sample prior and after each deposition step.

3.4.2. Photoelectrical method

In this work the vectorial photoinduced ET at the interface of semiconductor and organic D-A layer was studied by means of the time-resolved Maxwell displacement charge method, TRMDC [**41**] [**42**]. The measurements were carried out at room temperature and the samples were exposed to air.

Figure 3.3 presents a schematic view of the used instrument. The main components are a pulsed laser that provides the energy for the excitation, the sample, which is connected to a resistance and an amplifier, and a digital oscilloscope with a computer. The photo excitation is a short pulse coming from a titanium-sapphire laser CF125 [**43**] capable of producing pulses at 350-440 or 700-880 nm with durations of 10-20 ns and energy in the range 1-50mJ.
This laser is pumped by the second harmonic of a Q-switched Nd:YAG laser LF117 [**43**] that produces 5-20 ns pulses at 1.06 μm or 532 nm with energy up to 200 mJ [**44**]. The signal is registered by a TDS3032B oscilloscope, 300 MHz, 2.5 GS/s, with 2 channels [**45**].

The sample is placed in a metallic box, Faraday cage, which prevents the contamination of the signal originated in the plate. The glass side of the plate is exposed to the laser beam and is perpendicular to it; the ODA side is in touch with a metallic drop. A metallic clip both keeps the sample in place and provides electrical contact between the sample, the amplifier, the input resistance and the oscilloscope. The ITO layer of the sample works as first electrode. The second electrode is a circular area, approximately 1 mm diameter, created by the contact of the ODA side of the plate with the metallic drop, indium-gallium alloy.

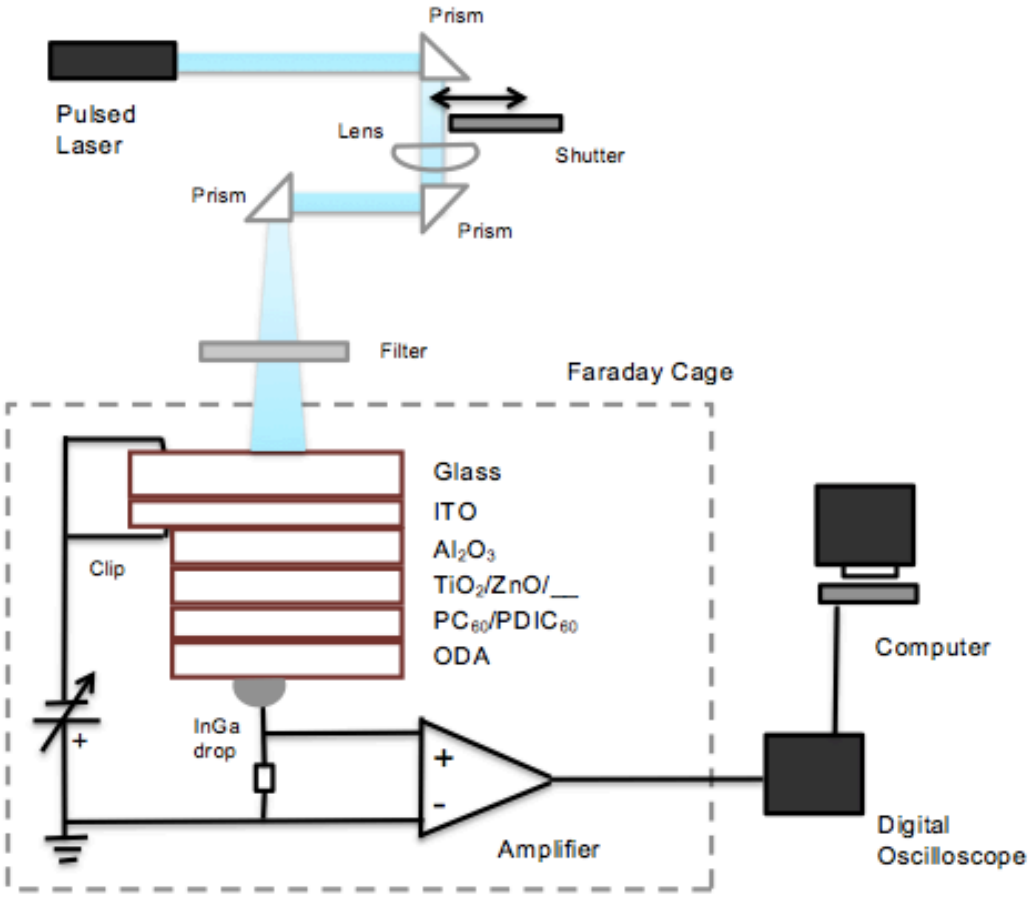

Figure 3.3 *Schematic presentation of the TRMDC instrument. A metallic clip keeps the sample in a position so that the light enters from the glass side and completely illuminates the InGa drop.*

This set up can be modelled with a RC circuit where R is the amplifier input resistance and C is the capacitance given by the sample.
The ODA and $\mathbf{Al_2O_3}$ insulating layers surrounding the active one, (dyad layer or semiconductor-dyad bi-layer) guarantees that the observed signal is produced by the electrons moving in the active layer only. Control measurements were carried out to confirm this hypothesis.

Once the light pulse strikes on the sample a charge separated state is formed at the semiconductor – active layer interface; charges can move in the active layer and then recombine. This process produces a rising signal, corresponding to the formation of the charge separated state (CS), and a decay, relative to the charges recombination. The positive or negative value of the signal is determined by the direction of the moving electrons: for these samples a positive one corresponds to electrons flowing from the metallic drop to the ITO and vice versa. The intensity of the signal is directly proportional to the amount of CS states and to the charge displacement.

This method investigates only the vertical movement of the charges, perpendicularly to the electrode, and does not provide any information regarding the lateral one. In addition no distinction can be done between anionic and cationic movement unless time-resolved spectroscopic methods are used [**46**].

For this work a liquid InGa alloy was used as second electrode and the input resistances were 100 MΩ and 10 GΩ.
Samples containing **PC_{60}** as active layer were excited at 424 nm, 425 nm and 428 nm whereas samples containing **$PDIC_{60}$** at 700 nm. Reference samples without organic layers were excited at 427 nm, 428 nm and 701 nm.
The used energy densities were in the 0,5-1,5 mJ/cm^2 range and a series of neutral density filters was used to adjust the energy.
External bias voltage equal to ± 400 mV, -600 mV and -1 V were applied to study the free charge motion if such effect exists.
Measurements were carried out in the photo-voltage mode that is working in time domains shorter than the instrument time constant. In this condition the amplitude of the signal is proportional to the density of CS states and the measured voltage change due to the current flowing in the circuit can be neglected.

4. Results and discussion

In this chapter the most relevant results of the work done are presented and commented. At first the absorption properties of each compound are introduced together with their π-A isotherm. The monolayer and multilayer absorption is then discussed. Finally the results obtained from the photo-voltage measurement are presented and critically analysed.

4.1. Solution characterization

Each used compound was characterized in solution before being used for thin film deposition. The absorption spectrum was measured and used as a reference, in terms of peaks position, for the subsequent film spectra. The π-A isotherm was determined and used to estimate the target pressure for the LB depositions.

4.1.1. Absorption spectrum

Figure 4.1 shows the absorption spectra of the used stock solutions after 100 times dilution, being respectively **CPTPP -** 0,0044 mM, **PC_{60}** - 0,0038 mM and **$PDIC_{60}$** - 0,0041 mM. All compounds were dissolved in chloroform.

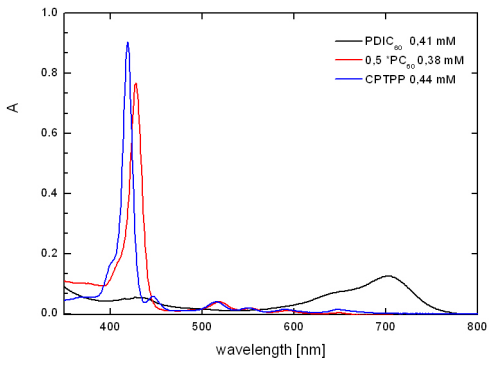

Figure 4.1 *Absorption spectra of CPTPP, PC_{60} and $PDIC_{60}$ stock solutions diluted 100 times.*

As expected [**47**] for **CPTPP** and **PC_{60}** the Soret band is clearly visible at 400 nm and the Q bands at longer wavelengths. To be precise the main maximum for **CPTPP** is located at 420 nm and the secondary peaks at 515 nm, 550 nm, 590 nm and 648 nm. For **PC_{60}** the peaks position is red shifted by few nanometres.

The fullerene signal [**48**] in **PC_{60}** is less visible due to its lower intensity as compared to the intensity of the porphyrin in the blue part of the spectrum. For **$PDIC_{60}$** dyad a broad band at 600-800 nm reflects the presence of the PDI and the bands at shorter wavelengths originate both from the fullerene and the PDI chromophores. [**24**]

4.1.2. Isotherm characterization

Figure 4.2 shows the isotherms of the organic compounds. The estimated target pressure values for the films depositions, i.e. the points with the highest slopes, are 8 mN/m for **CPTPP** and 7 mN/m for **PC_{60}** and **$PDIC_{60}$**. These values correspond to the surface pressure value for which a condensed and ordered floating film on the buffer layer is formed. In other words when the pressure reaches those values the film can be transferred over a solid support.

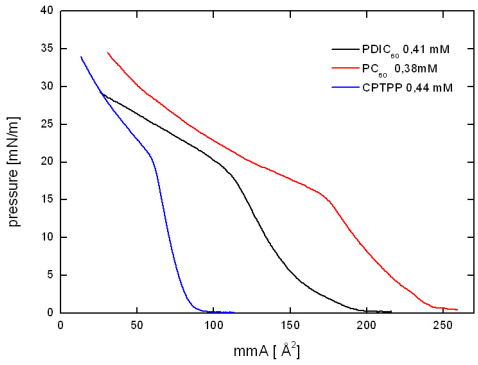

Figure 4.2 *Full isotherms of free-porphyrin, porphyrin-fullerene dyad and PDI-fullerene dyad on MQ water sub-phase.*

The mean molecular areas were 113 Å^2, 215 Å^2, and 259 Å^2, for the free porphyrin, the porphyrin-fullerene dyad and the PDI-fullerene dyad, respectively. These values are reliable estimations of the surface area occupied by the each single molecule for which all the floating molecules can be considered to be in the expanded-liquid phase [**49**].

4.2. Monolayer absorption

The formation of monolayer organic films was studied on different substrates and their stability and quality, in term of transfer ratio and absorbance, were checked. The deposition of these films was necessary to have a reference for the complex structures formed by organic dyads on ALD semiconductors.

The choice of the deposition technique of the organic films, either LB or SAM, was ruled by the specific aim of each plate and by the possible presence of semiconductors layers.

In particular LB was used for the deposition of organic monolayers directly on glass that did not require any coating onto the film itself. The presence of additional layers would have induced the breaking of the fragile monolayer.

The determination of the transfer ratio provided reliable information regarding the packing density of the monolayers. The absorbance values of LB monolayers were used as reference value for flat monolayers.

SAM technique was used for depositions on semiconductor layers, ZnO and TiO_2, and on insulating layers, Al_2O_3. The higher stability of SAMs allowed the formation of multilayer structures. On the contrary to LB films, the quality of SAMs could not be easily checked via the transfer ratio but only more qualitatively via spectroscopic measurements.
Each compound was thus first deposited via the LB technique in order to obtain an estimation of the mean molecular area and to gather information about the quality of the film. Dipping the substrate in an adequately concentrated solution was then carried out, that is what in this work is called dipping SAM.
Here the monolayer absorption of CPTPP and of the dyads films deposited on **G**, **G|ZnO** and **ITO|ZnO** supports via LB, LS and dipping SAM are reviewed. Comparisons are made in term of transfer ratio and absorbance value; the reliability of the used techniques is also considered.

4.2.1. CPTPP monolayers

Free base porphyrin was deposited on glass plates via LB and LS techniques; the corresponding monolayer absorption spectra are presented in Figure 4.3a. Conflicting results emerged from the LB film deposition on glass: a satisfactory absorption, A = 0,022, and a very low TR value, TR=0,012. Since the LB monolayer is formed on both sides of the plate and the spectrophotometer detects the presence of both monolayers the absorption of a single CPTPP monolayer on a glass substrate is equal to A = 0,011. The lower TR obtained led to the assumption that a loose packed monolayer was formed on the glass support.

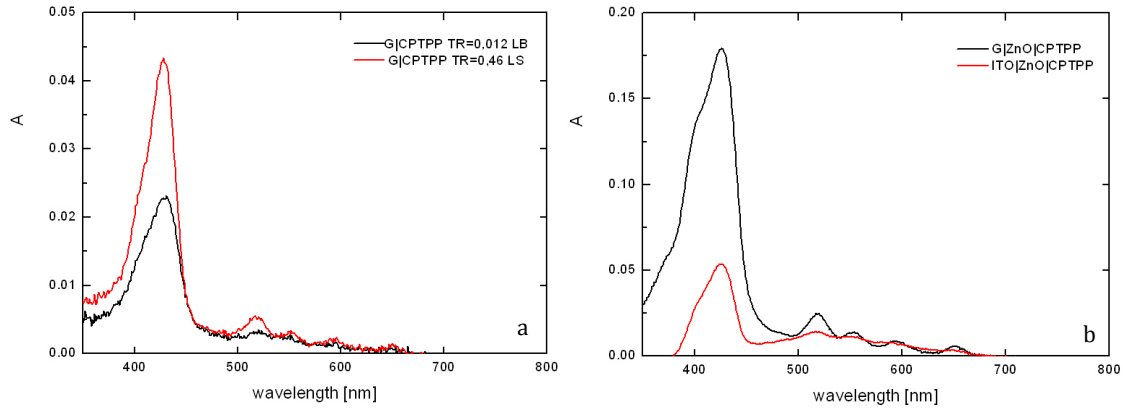

Figure 4.3 *a) CPTPP monolayers absorption on G via LB and LS techniques b) CPTPP monolayer absorption on G|ZnO and ITO|ZnO via dipping SAM.*

LS deposition was then carried out to verify the molecules adhesion on the glass support. Better results in term of absorption were obtained as shown in Figure 4.3a, red line; the absorbance was equal to A=0,043, for a single monolayer, and the manually calculated TR value was TR=0,46. This confirmed the **CPTPP** transfer from the floating film to the glass substrate.

The orientation of the porphyrin molecules is opposite for the LB and LS film as presented in Figure 4.4. When the **CPTPP** molecules are spread on the water surface they tend to orientate so that the hydrophilic carboxylic group is in the water and the porphyrin hydrophobic part is atop of the layer.
For LB deposition from solution to air the **CPTPP** will anchor on the glass plate with the carboxylic group; for LS depositions the plate will be in contact with the phenyl group opposite to the carboxylic one.

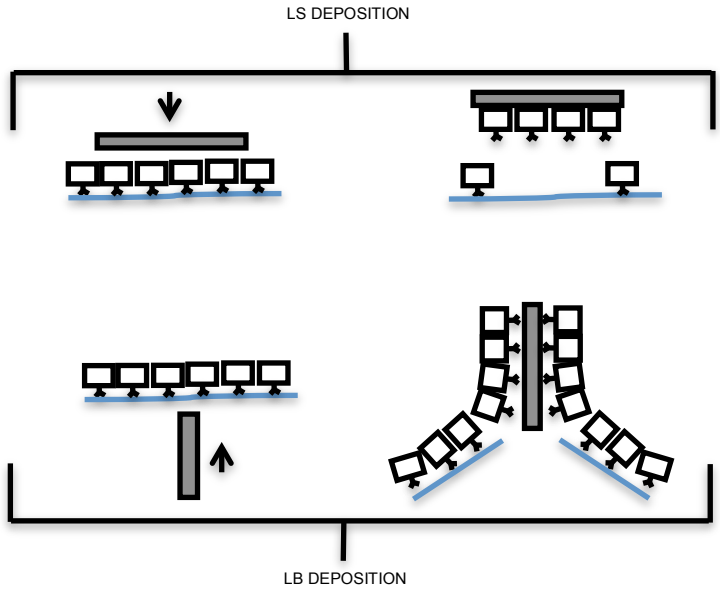

Figure 4.4 *Schematic presentation of the porphyrin attachment on the plate in LS and LB deposition. In the first case the carboxylic group is exposed on the surface of the thin film, in the second one is the anchoring group for adhesion on the plate*

The LS film is deposited on one side of the substrate only whereas for LB film is deposited on both sides of the plate. Therefore the results of LS deposition can be considered as a better reference for CPTPP monolayer absorption.
Despite this positive outcome, the reproducibility of the LS technique was quite low. The TR value was only roughly estimated from the barrier displacement and each deposition was highly influenced by the manual skills of the person carrying it out. The subsequent depositions were carried out via LB technique due to the higher reproducibility of this technique over LS one.
For both depositions the porphyrin Soret band broadened and shifted to higher wavelengths as compared to that of the **CPTTP** in solution. This phenomenon could be caused by the porphyrin aggregation in the solid film [**19**].

In Figure 4.3b the results of the SAM deposition on **G|ZnO** and **ITO|ZnO** substrates are presented. The absorption maxima are 0,179 and 0,053 for **G|ZnO** and **ITO|ZnO,** respectively. The higher absorption of the layer on the zinc oxide support may be due to the morphology of the **ZnO** spin coated film and in particular to the different surface roughness, which can have influenced the

measured absorption of organic molecules. Peak broadening and shifting to red part of the spectrum is observed also for these films.

4.2.2. PC_{60} monolayers

Figure 4.5a presents the absorption of LB **PC_{60}** monolayers on **G** and on **G|ZnO**. The transfer ratio of the sample deposited on glass substrate was 0,56 and the absorption intensity of this sample, A=0,04 for two monolayers, is in agreement with the transfer ratio. A=0,02 will be the reference absorbance value for one flat porphyrin-fullerene monolayer on **G.** For **G|ZnO** sample the transfer ratio was 0.008 only. In spite of the low TR value, some molecules were deposited as well, but considering possibly high roughness of the **G|ZnO** substrate no reliable conclusion can be done on the density of molecules on the surface. The absorption intensity for the Soret band is equal to A=0,017.

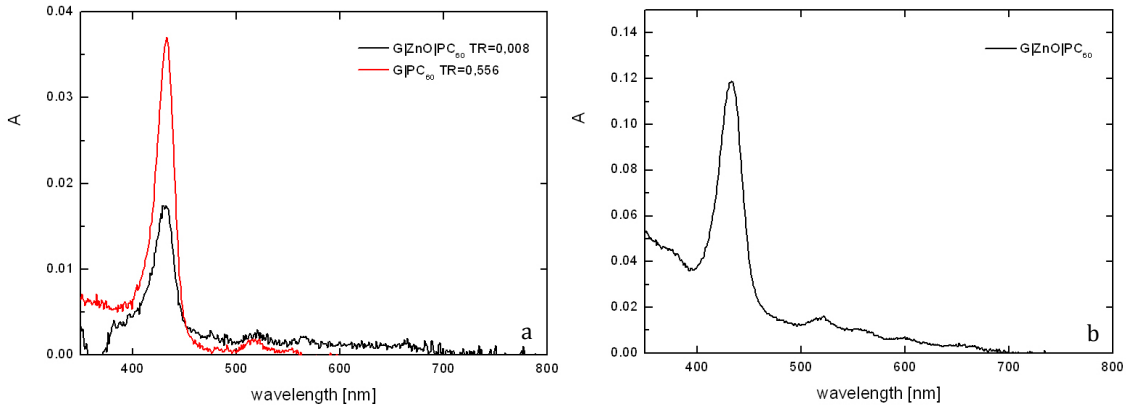

Figure 4.5 *a) PC_{60} monolayers absorption on G and G|ZnO via LB technique b) PC_{60} monolayer absorption on G|ZnO via dipping SAM.*

Dipping SAM on **G|ZnO** gave an absorption value equal to A=0,11 at the Soret band as Figure 4.5b depicts. This value is one order of magnitude higher than the one obtained for the LB deposition of **PC_{60}** on the same type of substrate, **G|ZnO.** It can be thus indicative of a denser film. Comparing this absorption value with the one of the **CPTPP** SAM on **G|ZnO,** this last deposition can be considered a successful one. On equal deposition techniques and conditions the quality of **CPTPP** and **PC_{60}** monolayers can be considered similar. This implies that the fullerene presence does not decrease the density with which the porphyrin molecules form a monolayer.

It is important to note that for **CPTPP** films the porphyrin linked to the ZnO substrate using the carboxyl group, whereas for **PC_{60}** film the fullerene holds the anchoring group. It can thus be assumed that the porphyrin is atop the fullerene molecules in this type of monolayer structure.

4.2.3. $PDIC_{60}$ monolayers

The results of **$PDIC_{60}$** depositions are presented in Figure 4.6. Very low absorption values were obtained for LB films on **G** and on **G|ZnO,** Figure 4.6a. This result is in agreement with the absorption spectrum of the **$PDIC_{60}$** solution.

A first LB deposition on a glass support gave promising results: the transfer ratio value was equal to 1,009 and the absorbance at 700 nm was equal to 0,006.
A second deposition on a more rough substrate, **G|ZnO**, gave an unexpected low value of transfer ratio, TR=0,065. A slight lower absorbance, as compared to the one of the first deposition, was registered.
Since the roughness of the spin coated zinc oxide layer is higher than the one of the glass substrate, higher absorbance values were expected for the **$PDIC_{60}$** monolayer on the semiconductor support. The **$PDIC_{60}$** deposition on **G|ZnO** is thus considered as an unsuccessful one.

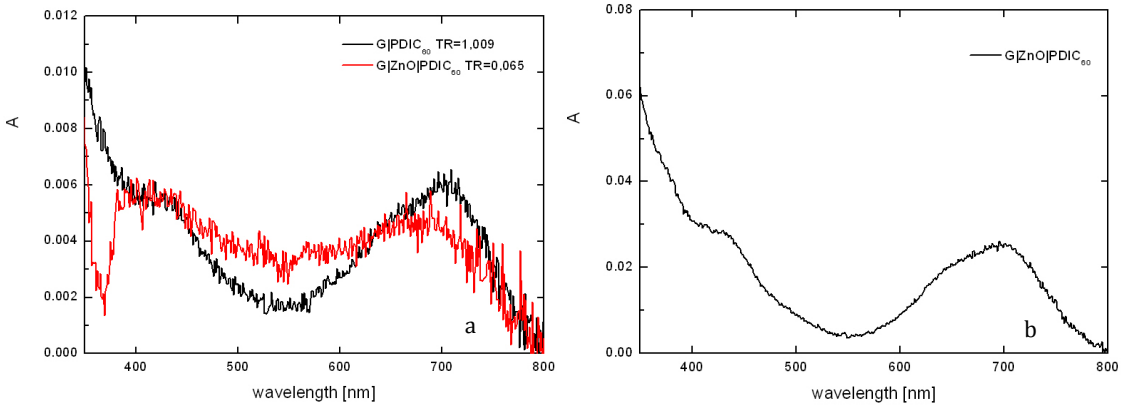

Figure 4.6 *a) $PDIC_{60}$ monolayers absorption on G and G|ZnO via LB technique b) $PDIC_{60}$ monolayer absorption on G|ZnO via dipping SAM.*

The deposition via dipping SAM on **G|ZnO,** Figure 4.6b, gave more promising results being the obtained absorbance value, A=0,025, one order of magnitude higher than the one obtained on the same type of substrate via LB.
The main conclusion is that **$PDIC_{60}$** films can be successfully deposited by dipping SAM method on relatively rough surfaces of ZnO layers on glass.

The short contact time between the solid support and the molecules of the floating film in the LB technique does not leave time for the molecular rearrangements, if necessary. Defects in the film due to detached molecules from the film during the lifting movement or a not optimal arrangement of the molecules cannot be removed. Re-immersing the film in the trough would create a second layer of molecules but not cure those defects. On the contrary dipping SAM allows the curing of the pre-cited defects on a higher degree due to its different working principle. Since the plate is immersed in the solution for a long period of time the

molecules can organize themselves so that the least energetic, and thus the most compact, film is formed. Lifting the plate up at the end of the process does not induce the removal of the chemically adsorbed molecules on the solid support. For this reason the dipping SAM was the chosen technique to deposit the active layer of the photo-voltage samples.

4.3. Multilayer absorption

In this section the deposition of the previously studied dyad compounds, **PC_{60}** and **$PDIC_{60}$**, on semiconductor oxides layers formed via ALD is presented and commented. Promising results were obtained for the porphyrin-fullerene dyad while not completely satisfactory ones for the PDI-fullerene dyad.

4.3.1. PC_{60}

Deposition of dipping SAMs of **PC_{60}** on semiconductor substrates was carried out with satisfactory results. Figure 4.7a shows the change in monolayer absorption with the immersion time for the **Al_2O_3**, **ZnO** and **TiO_2** plates. The measured absorption values, at 1 hour immersion time, were comparable with the reference absorbance value, A=0,02, of **PC_{60}** on **G** support. This means that the ALD oxide layers have a roughness comparable to the polished glass plate one. In particular **TiO_2** plates seems to have the smoothest surface, followed by **Al_2O_3** and **ZnO,** being the absorption values equal to 0,02, 0,025 and 0,055, respectively.
The different absorbance values may also be the result of different monolayer densities on the available substrates. The higher the organic film density the more intense will be the absorbance under comparable experimental parameters.

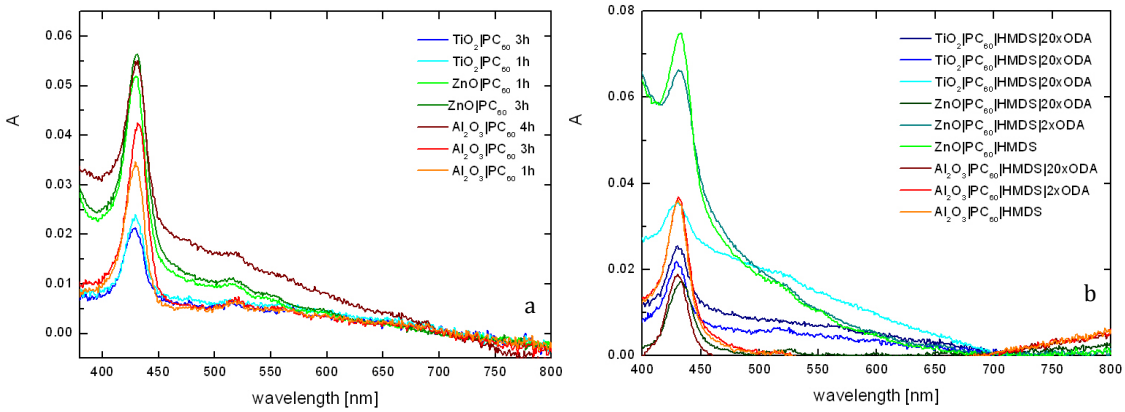

Figure 4.7 *a) Absorption spectra of PC_{60} monolayers on semiconductor substrates. The change in absorption with immersion times is indicated by the colours gradient. b) Change in absorption due to the hydrophobic treatment and the deposition of 20 ODA layers*

As inferred from the graph there is only a slight increase in the peak intensity upon increasing the immersion time from 1 hour to 3 or 4 hours. For this reason the monolayer formation can be considered to be complete already after 1 hour.
The immersion times needed to form a complete **PC_{60}** monolayer on ALD substrates are quite in agreement with the time needed to form the same film on polished glass and on spin-coated zinc oxide layer. This time is in the range 40 min-4 h. Despite this, the minimum immersion time changes with the nature of the substrate and with its morphology. Shorter immersion times are required for alumina than for titanium to obtain the same absorbance value and for zinc oxide spin coated substrates than for ALD ones.

Figure 4.7b presents the change in absorption of the plates due to the hydrophobic HMDS treatment and due to the deposition of the 20 insulating ODA layers.
A remarkable change in the scattering level was observed for each sample at high wavelengths due to the presence of the HMDS layer. This made the data analysis more difficult but general trends could be inferred anyway.
The change in absorption due to the deposition of ODA layers was monitored after 2 layers and at the end of the process. Though a general decrease in absorption was observed, the porphyrin-fullerene dyad presence is still confirmed by the absorption graphs in Figure 4.7b.

4.3.2. $PDIC_{60}$

Absorption data relative to **$PDIC_{60}$** dyad deposited on ALD semiconductor supports are presented in Figure 4.8a. All plates show very low absorption values. In particular no reliable signals were registered for **Al_2O_3** and **TiO_2** substrates. For the former the absorption signal did not present any typical features of the **$PDIC_{60}$** spectrum and for the latter a partly negative absorption was registered after a prolonged immersion in the solution. Extended immersion times, up to 20 hours, did not bring any remarkable increase in the absorption values.
The deposition of organic compounds on this type of substrates was unsuccessful since the presence of the **$PDIC_{60}$** could not be confirmed. Therefore these two samples were not used for the photo voltage measurements. On the contrary the absorption spectrum for **$PDIC_{60}$** on **ZnO** showed the expected features of the PDI-fullerene dyad and thus it was further manufactured to obtain a photo-voltage sample.

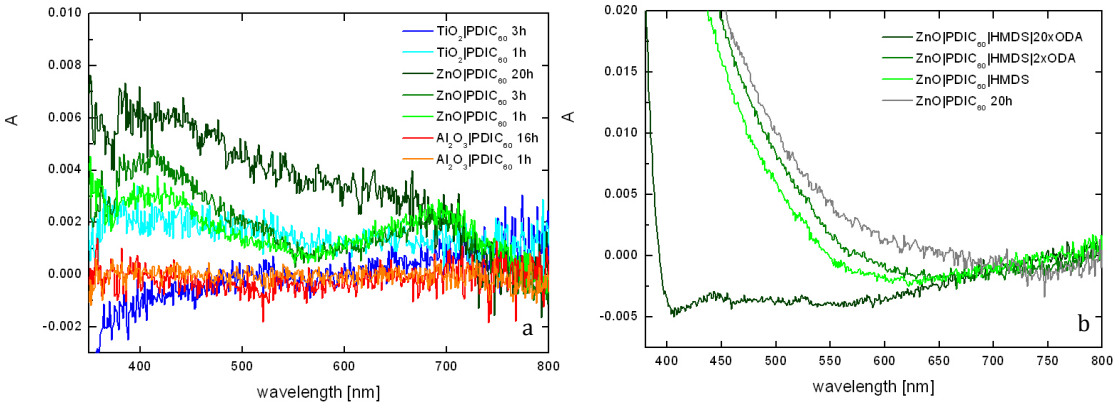

Figure 4.8 *a) Absorption spectra of $PDIC_{60}$ monolayers on semiconductor substrates. The change in absorption with immersion times is indicated by the colours gradient. b) Change in the scattering layer for ZnO|$PDIC_{60}$ sample after the hydrophobic treatment.*

Figure 4.8b shows the evolution of the absorbance of the **ZnO|PDIC$_{60}$** after the hydrophobic treatment. The deposition of the ODA layers by LB technique did not affect much the signal at longer wavelengths but at shorter the measured absorption is gradually smaller after the deposition, which was attributed to smaller light scattering due to "smoothing" effect of multilayer LB.

4.4. Photo-voltage measurement

The photo-voltage measurements carried out in this Thesis are a powerful tool to determine the behaviour of D-A pairs upon illumination and the influence of a semiconductor layer on the signal response.
In this section the obtained results are presented and investigated with the aim to get both qualitative and quantitative information.

For all the analysed plates a positive signal was obtained as a response to the photo excitation; this means that the relative orientation of the donor and of the acceptor moieties, with respect to the substrate, is the same for all the samples as well as the direction of movement of the electrons. The acceptor moiety, C_{60}, is anchored to the oxide layers whereas the donor one, either PDI or P, is closer to the ODA layers. As expected, upon illumination the electron transfer occurs from either PDI or P towards C_{60}.

4.4.1. Substrate effect

The acquired signal can be considered as completely originated from the active layer. Reference samples, without any organic layer, were tested in analogous experimental conditions as the real samples ones, and at higher excitation energy density values, to determine the possible presence of a signal produced by the

oxide layers. Figure 4.9 shows an example of the data obtained in this series of measurements.

ZnO|PDIC$_{60}$ excited at 4μJ/cm^2 produces a voltage of the order of tens of milli Volts at short and intermediate time scales, Figure 4.9a and Figure 4.9b, followed by an exponential decay at longer timescales, Figure 4.9c. The corresponding reference sample, excited at lower and higher energy density values, gave no response over the level of noise at all the tested time scales.

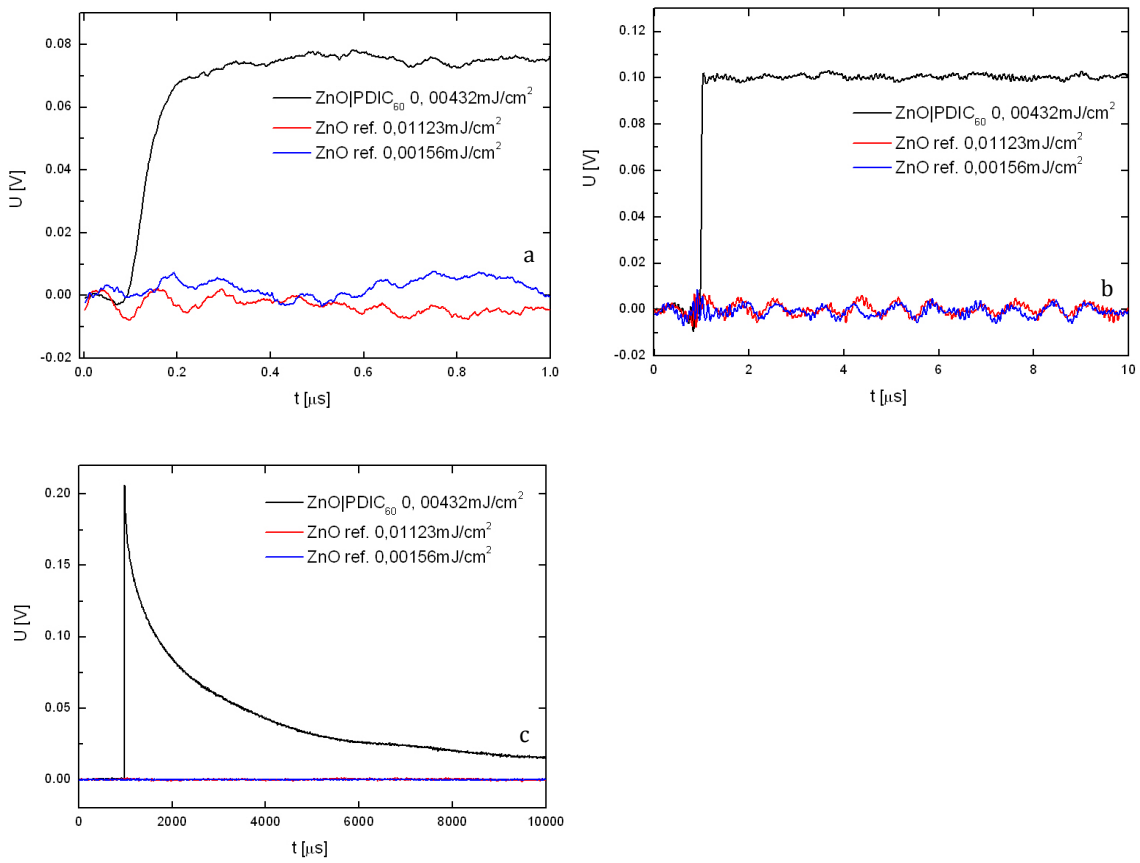

Figure 4.9 *Comparison of the signal originated by the reference sample, and by the sample with active layer. a) presents the short timescale response, b) the intermediate one and c) the long timescale response.*

The difference in the intensity of the responses and of the shapes, between the reference and the sample, justifies assignment of the response of the analysed sample as produced by the active layer only. The oxide layers contribution to the total signal can thus be neglected. This reasoning is still valid at higher excitation densities; at 10 μJ/cm^2 no response was registered for the reference plates. The corresponding graphs for the other studied samples are presented in Appendix A1. Application of an external voltage, equal to ± 400 mV, -600 mV and -1 V, did not alter the response of the reference samples, as reported in Appendix A1. No charges movement occurs then inside the reference samples in the experimental conditions used.

The **TiO_2** reference sample was the only exception since a low intensity and positive decay was observed both at short and long timescales and with a non-null applied voltage. Also in this case its presence was neglected, due to its low intensity as compared to the sample response one, and the total signal was considered as originated from the active layer only.

4.4.2. Oxide layer effect on PC_{60}

The influence of the oxide layer on the photo-voltage signal was investigated considering the sample with alumina oxide only as the reference one. This type of analysis was carried out only for the **PC_{60}** dyad due to the unsuccessful synthesis of **Al_2O_3|$PDIC_{60}$** and **TiO_2|$PDIC_{60}$**. Comparable energy densities values, of the order of 0,02-0,05 mJ/cm^2, were used to excite the different samples.
The signal obtained from **Al_2O_3| PC_{60}** can be considered as the pristine signal of the organic compound since the presence of alumina on one side of the active layer and of ODA on the other avoids any external interaction of the organic monolayer.

Figure 4.10 presents the signal obtained in the nanosecond, microsecond and millisecond time domain. For clarity of the comparison the curves were zoomed 10 and 0.1 times when necessary.

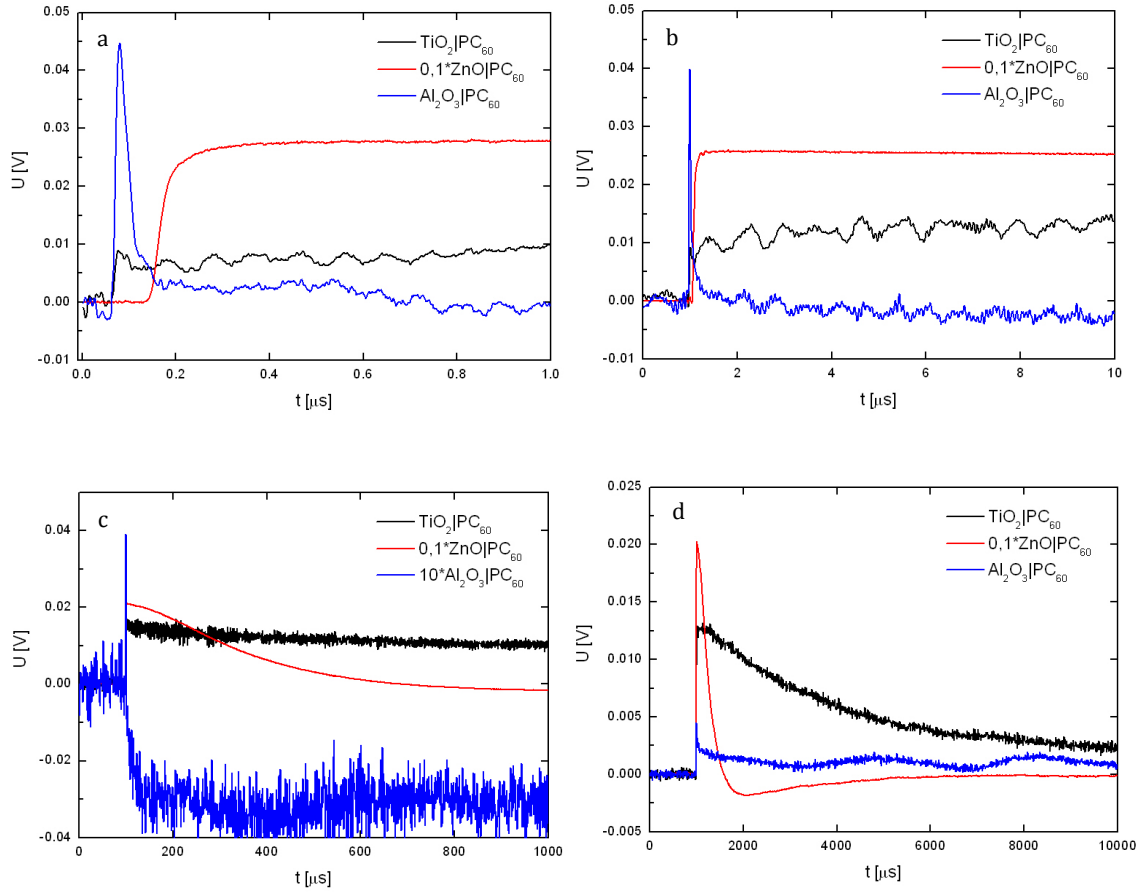

Figure 4.10 *Change in the shape of the response of PC_{60} samples due to the presence of ZnO or TiO_2 layers. Short time domains in a) and b) and long time scales in c) and d). The signal originated in the zinc oxide containing plate was divided by ten in each graph and the one originated in the alumina containing plate was multiplied by ten in graph c).*

The acquired transient voltage plots are a graphical representation of the electron transfer process between the organic layer and the semiconductor one.
Figure 4.11 briefly schematizes it. Before illumination the active layer is electrically neutral. After the photon absorption by one dyad molecule an intermolecular charge separated state is formed and a positive charge is localised on the porphyrin whereas a negative one on the fullerene. The electron is then transferred to the oxide layer and finally it will slowly recombine with the positive charge at the active layer-semiconductor interface.
In Figure 4.10 the CS formation is represented by the first part of the steep peak. The part of the response for which the voltage is reasonably constant with time represents the charge separated state with the electron localized in the oxide layer. The decaying part denotes the charge recombination process.

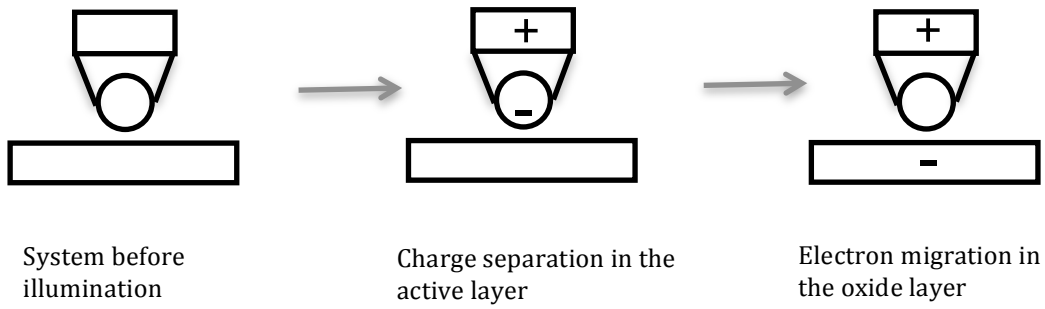

Figure 4.11 *Schematic view of the electron transfer process. The photon absorption by the dyad complex induces a positive charge on the porphyrin moiety and a negative one on the fullerene moiety. The electron can further migrate to the oxide layer before recombining with the positive charge.*

The formation of the CS state in **Al_2O_3| PC_{60}** and its recombination are limited to the ns domain. This means that both the processes are very fast and they take place in the active layer only. The signal is clearly visible at longer yet with a higher level of noise.

The addition of the zinc oxide and titania layer modifies the response of the dyad molecules both in its intensity and in its shape. The presence of zinc oxide enhances the signal in its intensity, up to one order of magnitude more, and increases gradually the charge recombination time. The formation of the CS state occurs in few nanoseconds after the excitation, Figure 4.10a, and is complete in few hundreds of microsecond after the excitation, Figure 4.10c. The recombination of charges, that is the decaying part of the curve, occurs few milliseconds after the excitation. The zinc oxide layer creates an additional electron acceptor layer. After the first charge separation in the active layer the electron is capable of moving into the bulk of the semiconductor thus generating a constant voltage with time. The recombination requires more time since the electron is not close anymore to the charged porphyrin. The ten times increase in the zinc oxide plate response as compared with thickness of ZnO film relative to the thickness of the donor-acceptor layer and suggests that the electron may diffuse into the bulk of the semiconductor layer.

The presence of the titania layer induces a phenomenon analogous to that one created by the zinc oxide layer since the charge recombination process is prolonged in a similar way. The intensity of the signal did not increase as much as in the case of the zinc oxide containing sample though. This may be caused by the presence of traps, close to the surface of the titanium dioxide layer, that limit the electron diffusion into the bulk of the film. Another possibility is the non homogeneous orientation of the dyad molecules on the titania surface; if the molecules lay on the surface, the porphyrin and the fullerene would be directly in touch with the semiconductor and the electron transfer process would be modified. The presence of additional charges on the titania surface may interfere

with the electron movement and induce different recombination processes thus affecting the photo-voltage signal intensity.

The different time domains shown in Figure 4.10 are a representation of the same phenomenon during its evolution; coherency in the peak intensity and shape evolution is thus expected. For measurements carried out in the same day this consistency was always observed; however for test carried out in different days this rule is not respected anymore. The different laser energy density and the non reproducible excitation spot size and location on the plate are possible causes. This is the reason for which the **Al_2O_3| PC_{60}** peak intensity in the millisecond domain differs from the one at shorter timescales.
Change of the curve shape was also observed for measurements carried out as long as one month later, leading to the assumption that samples alteration may have occurred. This hypothesis will be investigated later.

4.4.3. Time evolution of $PDIC_{60}$ signal

The evolution of the PDI-fullerene dyad signal is shown in Figure 4.12. The raising curve in the nanosecond domain, Figure 4.12a, represents the formation of the CS state. This part of the signal is comparable to the **PC_{60}** ones on ZnO substrate for its shape but not for its intensity. As expected from absorption measurements, **$PDIC_{60}$** signal intensity is one order of magnitude lower than that of **PC_{60}** one.
The recombination of charges occurs in the millisecond domain and it is indicative of a long-lived specie.

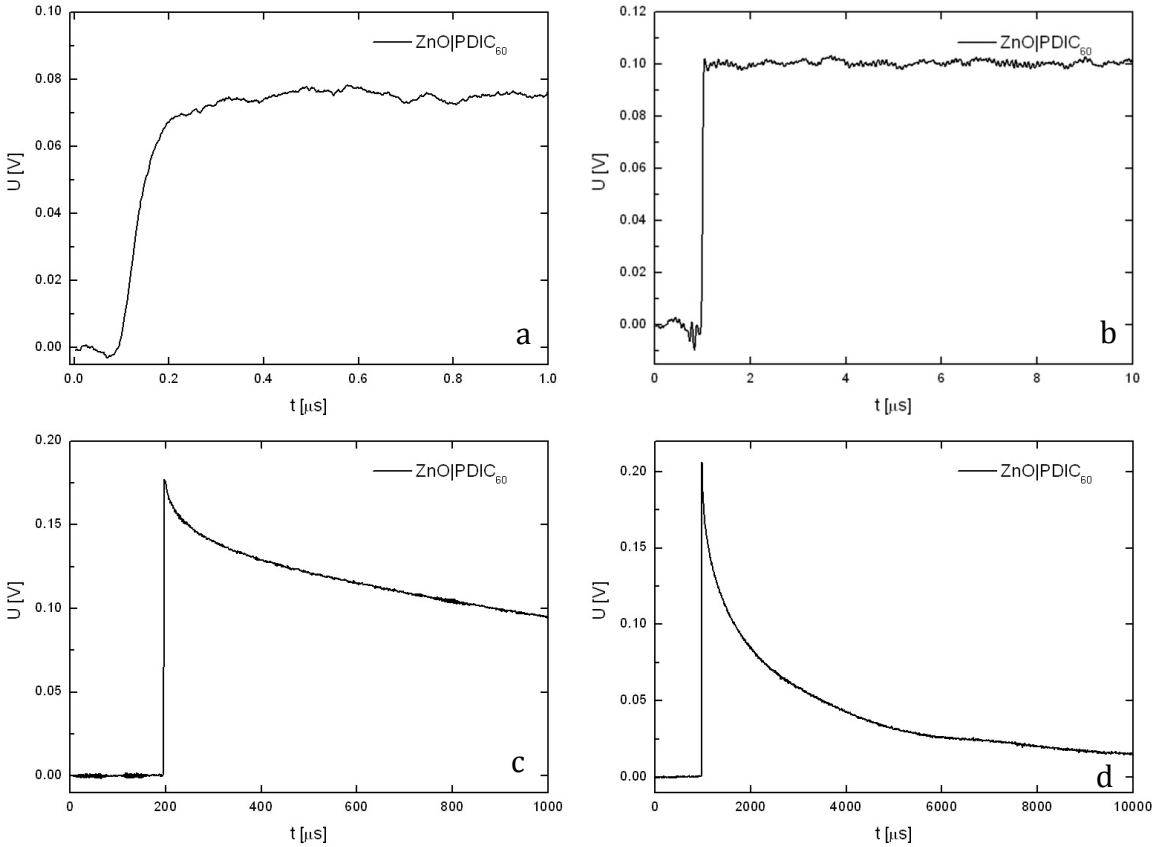

Figure 4.12 *Time evolution of the $PDIC_{60}$ signal on ZnO substrate at different timescales. a) and b) refers to the charge separation whereas c) and d) to the charge recombination process.*

4.4.4. Applied resistance effect

Tests at constant time scale and energy density, with a variable input resistance of the measurement circuit, 100 MΩ and 10 GΩ, were carried out. The aim was to determine to which extent the lifetime value of the photo-voltage response was influenced by the capacitance of the sample. Table 4.1 presents the results obtained using a bi-exponential fitting of the photo-voltage decays. Lifetime1 refers to a fast phase decay of the CS state and Lifetime2 to the slower charges recombination. In the case of **TiO_2** and **ZnO** samples the dominating is the long lived component whereas for **Al_2O_3|PC_{60}** sample the faster (Lifetime 1) is the dominant process. The charge separation phenomenon is not resolved at this long timescale. Generally, if the lifetime values at different resistances do not differ more than two times one from the other they can be considered to be equal. This would mean that there is no capacitance effect and the observed response is due to the organic layer only. Likewise if the difference in the fitted lifetimes values is not negligible the capacitance of the sample and input resistance of the amplifier should be taken into account to determine the real lifetime.

Table 4.1: *charge recombination lifetimes at 100 MΩ and 10 GΩ resistance*

Sample	**R = 100MΩ**		**R= 10GΩ**	
	Lifetime 1 [µs]	Lifetime 2 [µs]	Lifetime 1 [µs]	Lifetime 2 [µs]
Al_2O_3| PC_{60}	125	(2327)	145	(13026)
TiO_2|PC_{60}	120	1670	66	16355
ZnO|PC_{60}	59	6797	65	7143
ZnO|$PDIC_{60}$	__	7064	__	10043

Coherent behaviours were observed for **Al_2O_3** and **ZnO** containing samples whereas a different one for **TiO_2** sample. Figure 4.13a shows that increasing the input resistance of the circuit the measured decay lifetime increases for **TiO_2|PC_{60}**. This indicates that the higher resistance should be used to measure that charge recombination in this sample. At 100 MΩ the calculated lifetime was limited by RC of the measurement system, which is roughly 10 ms. At 10 GΩ the RC value is roughly 1 s, and the determined lifetime, 16 ms, can be attributed to the charge recombination in the sample.

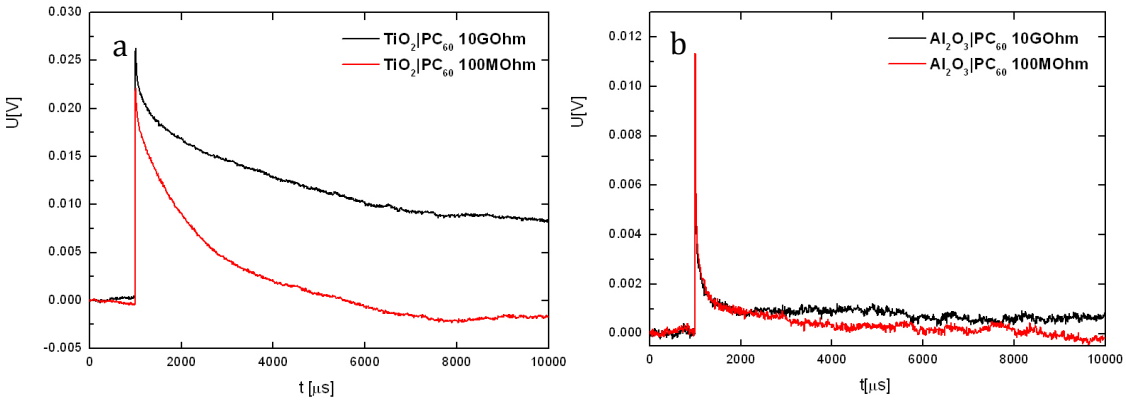

Figure 4.13 *Resistance effect on TiO_2|PC_{60},a), and Al_2O_3| PC_{60}, b).*

The high level of noise present at long timescales for the **Al_2O_3| PC_{60}** sample, Figure 4.13b, makes only the fast phase decay values meaningful. As it can be inferred from Lifetime1 values, there is no resistance effect on the charge recombination phenomenon.

Figure 4.14 presents the behaviour of **ZnO|$PDIC_{60}$** and **ZnO|PC_{60}** samples. Also for these samples the higher input resistance does not significantly affect the lifetime. Lifetime2 values are the only meaningful ones being the Lifetime1 ones too close to the resolution limit of the instrument and not always measurable.

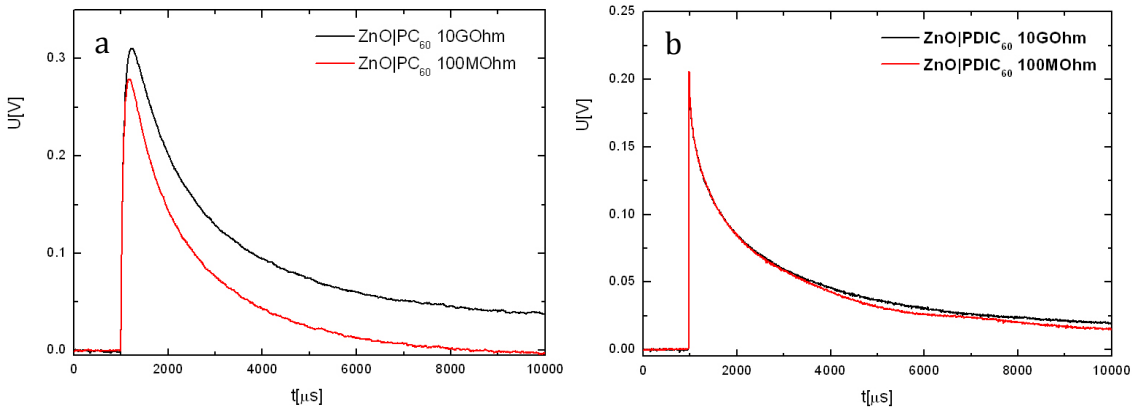

Figure 4.14 *Resistance effect on ZnO|PDIC$_{60}$ a), and ZnO|PC$_{60}$ b).*

It can thus be concluded that for **Al_2O_3| PC_{60}**, **ZnO|$PDIC_{60}$** and **ZnO|PC_{60}** samples the observed response is the real one of the sample with either input resistance used, whereas for **TiO_2|PC_{60}** there is a non negligible effect coming from the instrument RC, indicating that the higher input resistance has to be used to observe the real signal decay.

4.4.5. Energy density effect

The effect of the energy density of the laser on the intensity of the response was investigated. The samples were tested in the same experimental conditions with energy density variable in the range 0,004 mJ/cm^2 – 0,051 mJ/cm^2. For porphyrin containing dyads the critical value above which there is 50% of probability of excitation is approximately 1 mJ/cm^2. This means that for the used energy densities it is correct to assume that only a few dyad molecules get excited for each laser pulse. The dissociated electron will recombine with the positive charge left on the molecule the electron was originated from. No lateral interaction between that particular electron and another excited dyad molecule is assumed to occur. Increasing the energy density the number of excited dyad molecules will increase in a linear way. Figure 4.15 shows the plot of the peak intensity versus the energy density. The expected linear increase in the response upon increasing of the excitation density is observed.

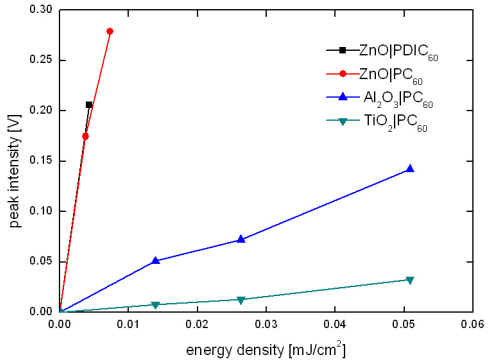

Figure 4.15 *Photo-voltage intensity response as a function of the laser excitation density. A linear behaviour is observed for all the samples, yet with a different rate.*

The relative increase in the signal changes from sample to sample due to the presence of different semiconductors layers. The slowest rise with the energy density is observed for **TiO_2|PC_{60}** whereas an intermediate one for **Al_2O_3| PC_{60}**. The steepest rise occurs for the **ZnO|$PDIC_{60}$** and **ZnO|PC_{60}**. No reasonable difference in the intensity of the rise was observed for **P** and **PDI** deposited on **ZnO** even though only partial data were acquired in this case.

4.4.6. Bias effect

Tests at non-null external voltage were carried out to observe the possible charges movement in the semiconductor layers of the samples. If charges movement in those layers is possible a change in the photo-voltage response should be observed. On the contrary, if the movement is not permitted, due to the presence of an insulating layer for example, no change in response should be observed upon variations of the external voltage.

Not coherent results are obtained for ZnO containing plates as shown in Figure 4.16. The expected change in the response is presented by **ZnO|PC_{60}** but not by **ZnO|$PDIC_{60}$**. In particular, when a positive voltage is applied to **ZnO|PC_{60}** the change in the response is minimum and when a negative voltage is applied the change is more remarkable. This means than the sign of the voltage can enhance or decrease the charges movement.

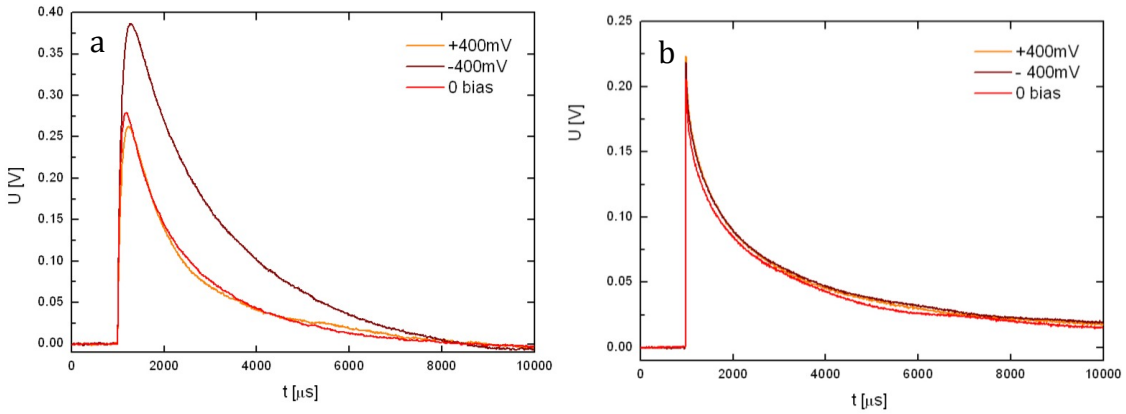

Figure 4.16 *Bias effect on ZnO|PC$_{60}$, a), and ZnO|PDIC$_{60}$, b). Charge movement is observed in the first case when a negative voltage is applied. No noticeable charge movement occurs in the second case.*

As expected, no change is shown by the **Al_2O_3| PC_{60}** response as presented in Figure 4.17a. Being alumina an insulating material no charge movement is allowed inside the layer. Figure 4.17b shows also an unexpected result for **TiO_2|PC_{60}**. Due to its semiconductor properties a charge movement is expected once a voltage is applied, yet no remarkable change was observed in the response. The presence of electronic traps inside the titania layer can be an explanation for this behaviour.

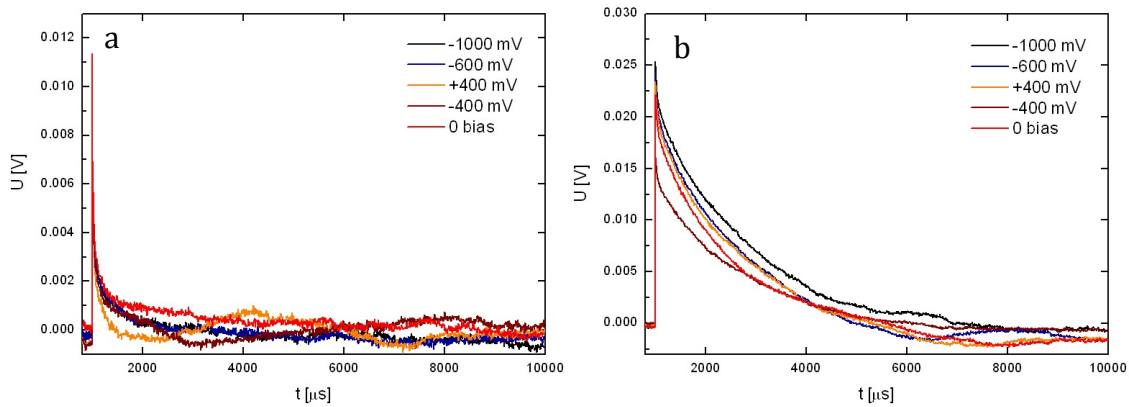

Figure 4.17 *Bias effect on Al_2O_3| PC_{60}, a), and TiO_2|PC_{60}, b). No charge movement is allowed by the alumina layer and, unexpectedly, by the titania one.*

4.4.7. Samples degradation

Not negligible changes in the samples response were observed during the several tests carried out; this led to the assumption that samples deterioration may have occurred.

The photo voltage graphs supporting this hypothesis are presented in Appendix A2 for **PC_{60}** samples. Similar energy densities were used to acquire the signal from the reference and from the samples in different days.

For all the samples a general decrease of the responses was observed for tests carried out one month after the first measures. **Al_2O_3|PC_{60}** intensity roughly decreased twice, **TiO_2|PC_{60}** intensity three times and **ZnO|PC_{60}** intensity six times.

The change in the shape of the response observed for **TiO_2|PC_{60}** sample is mainly due to the triggering of the measurement system.

Absorption measurements were carried out both prior and after the TRMDC measurements to verify the dyad presence on the samples. Appendix A3 presents the absorption spectra of each sample. No significant change in the Soret band absorption was observed for **PC_{60}** containing samples but a blue shift was recorded for all the peaks. Negligible changes in absorption were present for **ZnO|$PDIC_{60}$** sample.
This confirms the porphyrin and PDI presence in each sample but does not give information about the fullerene presence and its linkage with the donor moiety. The change in the response intensity could then be caused also by a change in the moieties arrangement due to the sample deterioration.

4.4.8. Source of errors

Since the properly setting of the TRMDC instrument required a not negligible amount of time it was not possible to carry out all the measurements on the same day. This inconvenience may have affected the quality of the obtained results due to the samples degradation with time and due to the variability of the laser setting.
The samples were stored in a dark and cool place in order to avoid the degradation of the porphyrin and the photo-activation of the titanium oxide; despite this, air contact and light may have deteriorated the active layer, both during the storage and the measurements.
The energy power of the Nd:YAG laser was influenced by slight temperature variations, affecting thus the energy of the beam impinging on the sample even for measurements carried out on the same day.
Even though particular care was paid, the excited area on the sample was not always the same and the calculation of the energy density introduced another error factor on the analysed data.
The multilayer structure was supposed to be made by uniformly organized molecules in each layer but this assumption could not be practically verified. It is thus possible that data from differently organized molecules were acquired without any potential distinction factor.
These practical factors decreased the precision of the results.

5. Conclusions

The main results of this Thesis can be summarized in the following way:

1. The absorption of organic dyad monolayers, **CPTPP**, **PC_{60}** and **$PDIC_{60}$**, on flat glass surfaces was studied via LB deposition. The absorbance values corresponded to films formed on both sides of the plates. The quality of the films in term of amount of molecules transferred to the substrate was monitored by recording the transfer ratio, (TR). Depositions were successful for **PC_{60}** and **$PDIC_{60}$**, but not for **CPTPP**. Attempts to use LB method for deposition of the same compounds on glass substrates covered with thin layer of **ZnO** were unsuccessful.

2. SAM depositions of **CPTPP**, **PC_{60}** and **$PDIC_{60}$** were carried out both on glass plates covered by a thin layer of **ZnO** prepared by spin-coating and annealing method, and on oxide films, **Al_2O_3**, **ZnO** and **TiO_2**, prepared by atomic layer deposition (ALD) method. The presence of the organic film on the substrate was confirmed by the absorbance values: being these values comparable to the values obtained via LB deposition on flat surfaces, for which TR was close to unity, it implies that a sufficient amount of molecules was transferred from the solution to the substrate. The sometimes higher absorbance values obtained for ALD films can be explained by the higher roughness of the latter compared to that of the spin-coated **ZnO** thin films. Satisfactory results were obtained for **PC_{60}** on all substrates whereas the deposition of **$PDIC_{60}$** was successful only on **ZnO** substrate.

3. The electron transfer process from the organic dyad to the oxide layer was studied by means of TRMDC technique. Partial results were obtained for **$PDIC_{60}$** due to the previous unsuccessful SAM depositions. Photo-voltage responses of **PC_{60}** dyad were studied on all supporting surfaces, **Al_2O_3**, **ZnO** and **TiO_2**, whereas for **$PDIC_{60}$** only on **ZnO** since the deposition on other oxides was unsuccessful. A very fast charge separation with short lifetime was observed for **Al_2O_3| PC_{60}** sample. This was considered as the pristine signal of the dyad monolayer in which the electron transfer takes place from porphyrin donor to fullerene acceptor, i.e. inside the organic layer only. The presence of additional semiconductor layers, **ZnO** and **TiO_2**, modified the electron transfer process. The charge separation is still a fast one whereas the charge recombination is much longer for both semiconductors. The photo-voltage response amplitude is increased by roughly ten times for **ZnO| PC_{60}** but somewhat lower for **TiO_2| PC_{60}** sample as compared to that of **Al_2O_3| PC_{60}**. This means that an efficient second electron transfer reaction takes place from the fullerene anion to the ZnO

layer thus resulting in roughly ten times longer separation distance between holes (porphyrin cations) and electrons (inside **ZnO** layer).

4. Long lifetimes for the charge separated state were observed for **TiO_2| PC_{60}** and **ZnO| PC_{60}** systems. This means that once the charge separation process has occurred in the active layer, the electrons can further move into the semiconductor layer thus prolonging the charge recombination time. The charges do not move freely in the multilayer structure but are most probably locally trapped as indicated by insensitivity of the photo-voltage response to bias voltage. The long-lived charge separated state makes these structures optimal for solar cells applications.

5. The main drawback of these multilayer structures with organic dyads as active layers is their stability. Degradations processes are assumed to occur since no coherency was observed in the photo-voltage data acquired as long as one month after the samples preparation. Better insulation form oxygen and other potentially harmful factors are thus required to improve durability of the devices.

Bibliography

1. Vivo, P.: Multicomponent molecularly controlled Langmuir-Blodgett systems for organic photovoltaic applications. J. Phys. Chem., 8559-8567 (2010)
2. Saarenpää H. Sariola, E.: Self-assembled porphyrins on modified zinc oxide nanorods: development of model systems for inorganic-organic semiconductor interface studies. The Journal of Physical Chemistry, 2336-2343 (2011)
3. Zhao, Z.: Metal oxide buffer layer for improving performance of polymer solar cells. Applied Surface Science, 6053-6056 (2010)
4. Photoinduced electron transfer. Mattay, J. , Berlin (1990)
5. Marcus, R.: Electron transfer reactions in chemistry: theory and experiment., Pasadena, USA (December 1992)
6. Bolton, J. R.: Basic electron-transfer theory. American chemical society, 7-23 (1991)
8. Allen, J. P.: Structure of the reaction center from Rhodobacter R-26: The cofactors. Proc. natn, Acad. Sci. U.S.A. , 5730-5734 (1987)
7. Moser, C. C.: Nature of biological electron transfer. Nature 355, 796-802 (1992)
9. Koeppe, R.: Photoinduced charge and energy transfer involving fullerene derivatives. Photochemical & Photobiological sciences, 1122-1131 (2006)
10. Green, M.: Solar efficiency tables (version 37). (2011)
11. Conibeer, G.: Third generation photovoltaics. Materials Today, 42-50 (2007)
12. Brown, G. F.: Third generation photovoltaics. Laser & Photonics Reviews, 394-405 (2009)
13. Po, R. In: AIM. (Accessed June 20, 2013) Available at: HYPERLINK "http://www.aim.it/" http://www.aim.it/
14. Su, Y.-W.: Organic Photovoltaics. Materials Today, 554-562 (2012)
15. Spanggaard, H.: A brief history of the development of organic and polymeric photovoltaic. Solar energy materials & solar cells, 125-146 (2004)
16. Vivo, P.: Multilayerred Thin Films for Organic Photovoltaics., Tampere (2010)
18. Porphyrins and metalloporphyrins. Smith, K. M., New York (1975)
17. D'Urso, A.: From self-assembly to noncovalent synthesis of programmable porphyrins' arrays in aqueous solutions. Royal Society of Chemistry, 8165-8176 (2012)
19. Takagi, S.: Porphyrin photochemistry in inorganic/organic hybrid materials: Clays, layered semiconductors, nanotubes, and mesoporous materials. Journal of Photochemistry and Photobiology, 104-126 (2006)
20. Josefsen, L. B.: Photodynamic therapy and the development of metal-based photosensitisers. (2007)
21. Fukuzumi, S.: Artificial Photosynthetic Systems Composed of Porphyrins and Phthalocyanines. In : The Porphyrin Handbook 8. Kadish, K. M. Smith, K. M. Guilard, R. , San Diego (2000) 115-152
22. Biesaga, M.: Porphyrins in analytical chemistry. a review. Talanta, 209-224 (1999)

23. Weil, T.: The Rylene Colorant Family—Tailored Nanoemitters for Photonics Research and Applications. Angewandte Chemie, International Edition, 9068-9093 (2010)
24. Dubey, R.: Synthesis and function of photoactive donor-acceptor systems of bay-functionalized perylene diimide dye in view of 1,7- and 1,6-regioisomers., Tampere (2013)
25. Imahori, H.: Porphyrin- and fullerene-based molecular photovoltaic devices. Advanced functional materials, 525-536 (2006)
26. Imahori, H.: Vectorial Electron Relay at ITO Electrodes Modified with Self-Assembled Monolayers of Ferrocene–Porphyrin–Fullerene Triads and Porphyrin– Fullerene Dyads for Molecular Photovoltaic Devices. Chem. Eur. J. , 5111-5122 (2004)
28. Krishnan, V.: Manipulation of thin film assemblies: Recent progress and novel concepts. Current opinion in colloid and interface science, 459-469 (2011)
27. Biswas, A.: Advances in top–down and bottom–up surface nanofabrication: Techniques, applications & future prospects. Advances in colloid and interface science, 2-27 (2012)
29. Otero, R.: Molecular self-assembly at solide surfaces. Advanced Materials, 5148-5176 (2011)
30. K. Sakakibara, J.: Thin-film-based nanoarchitectures for soft matter: controlled assemblies into two-dimensional worlds. Small, 1288-1308 (2011)
31. KSV NIMA. (Accessed June 13, 2013) Available at: HYPERLINK "http://www.ksvnima.com" http://www.ksvnima.com
32. Petty, M.: Langmuir-Blodgett films: an introduction. Cambridge University Press, Cambridge (1996)
33. Roberts, G.: Langmuir Blodgett films. Plenum Press, New York (1990)
34. Ritacco, H.: Monolayers and Multilayers Equilibrium and Mechanical Properties. In : Nanoscience Colloidal and Interfacial Aspects 147. Victor M. Starov, Leicestershire (2010) 649-695
35. Charitat, T.: Adsorbed and free lipid bilayers at the solid-liquid interface. The European Physical Journal B, 583-593 (1999)
36. Kaunisto, K.: Energy and electron transfer in organic multilayered thin films containing oriented porphyrin-fullerene dyad., Tampere (2009)
38. Fülöpa, E.: Langmuir–Blodgett films of gold/silica core/shell nanorods. Thin Solid Films, 7002-7005 (2012)
37. Massey, M. K.: The electrical and optical properties of oriented Langmuir-Blodgett films of single-walled carbon nanotubes. Carbon, 2424-2430 (2011)
39. Kafi, A. K. M.: Fabrication and electrochemical characterization of HRP-lipid Langmuir–Blodgett film and its application as an H2O2 biosensor. Thin Solid FIlms, 3641-3645 (2006)
40. Laurell, T.: Spin coaters and spin processors. In: Laurell Technologies corporation. (Accessed June 13, 2013) Available at: HYPERLINK "http://laurell.com" http://laurell.com
41. Tran-Thi, T.-H.: Photophysical, photoelectrical and non-linear optical properties of porphyrin-phthalocyanine assemblies in Langmuir-Blodgett

films. Thin Solid Films, 8-13 (1996)

42. Ikonen, M.: The photovoltage signals of bacteriorhodopsin in Langmuir–Blodgett films with different molecular orientations. Adv. Mater. Opt. Electron (1993)
43. Sol Instruments Ltd.: Sol Instruments. (Accessed June 13, 2013) Available at: HYPERLINK "http://solinstruments.com/en/" http://solinstruments.com/en/
44. Nanosecond Laser System. In: Labman. (Accessed June 13, 2013) Available at: HYPERLINK "http://labman.me.tut.fi/instruments/" \l "ns_lasers" http://labman.me.tut.fi/instruments/#ns_lasers
45. Tektronix Inc.: Oscilloscope. In: Tektronix. (Accessed June 13, 2013) Available at: HYPERLINK "www.tek.com/oscilloscope" \l "all" www.tek.com/oscilloscope#all
46. Vuorinen, T.: Photoinduced interlayer electron transfer in alternating porphyrin-fullerene dyad and regioregular poly(3-hexylthiophene) Langmuir-Blodgett films. Journal of Photochemistry and Photobiology, 185-191 (2005)
48. Ajie, H.: Characterisation of the soluble all-carbon molecules C60 and C70. Journal of Physical Chemistry, 8630-8633 (1990)
47. Prahl, S.: PhotochemCAD. In: Biomedics optics in Portland. (Accessed June 22, 2013) Available at: HYPERLINK "http://omlc.ogi.edu" http://omlc.ogi.edu
49. Oliveira, O.: Langmuir-Blodgett films-Properties and possible applications. Brazilian Journal of Physiscs, 60-69 (1992)

Appendix

A1 Reference samples photo-voltage spectra

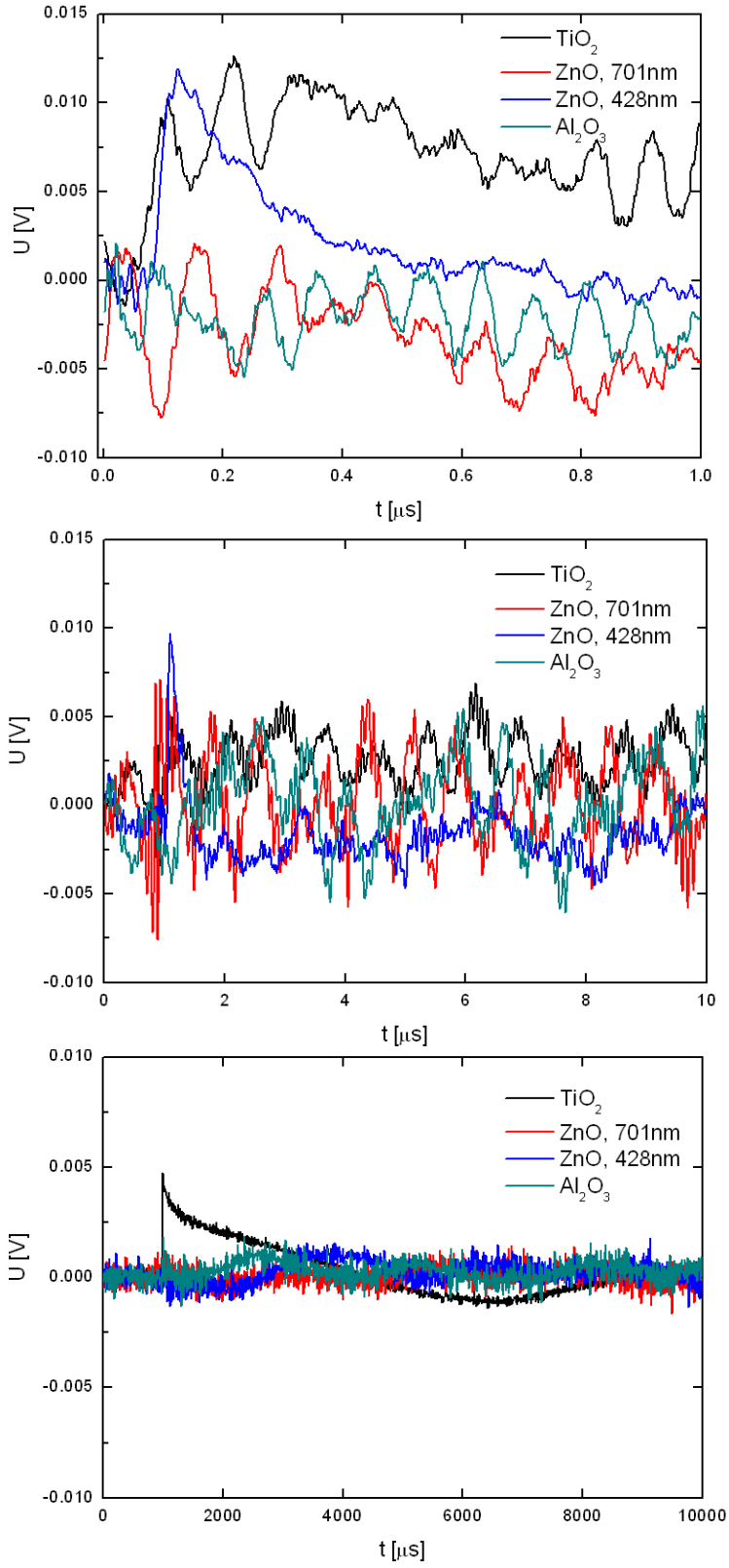

Photo-voltage response of the reference samples with variable applied voltage from +400 mV to -1000mV. From up to down, the response of the alumina, zinc-oxide and titania reference samples.

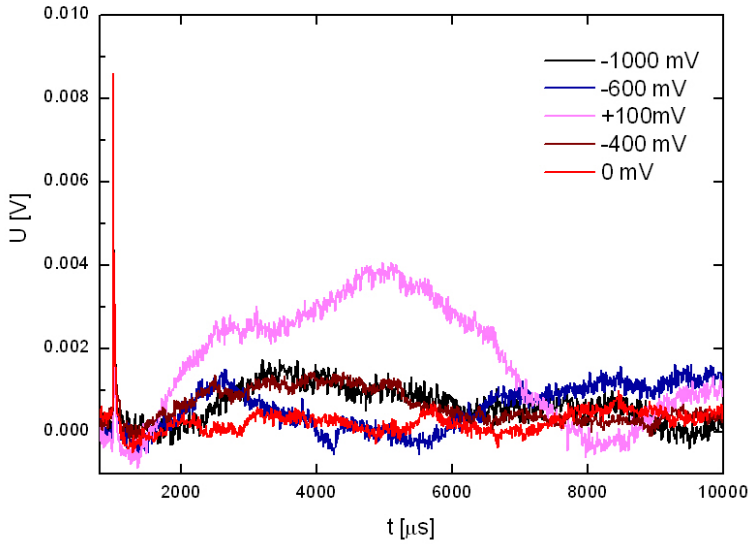

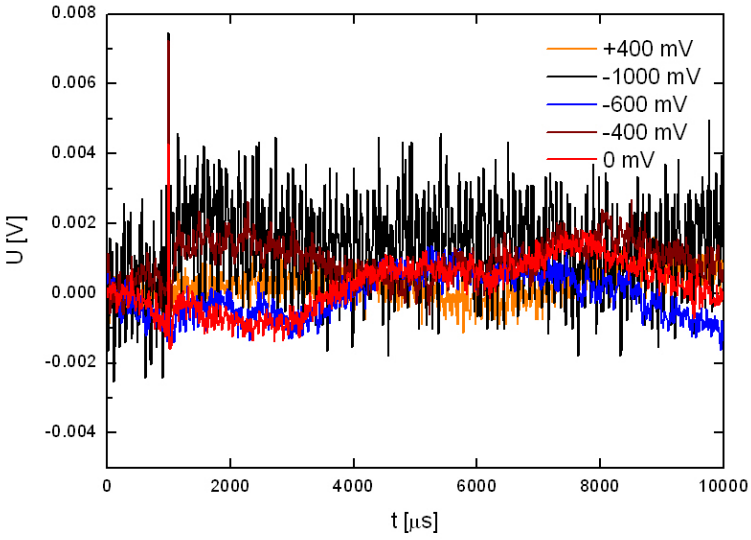

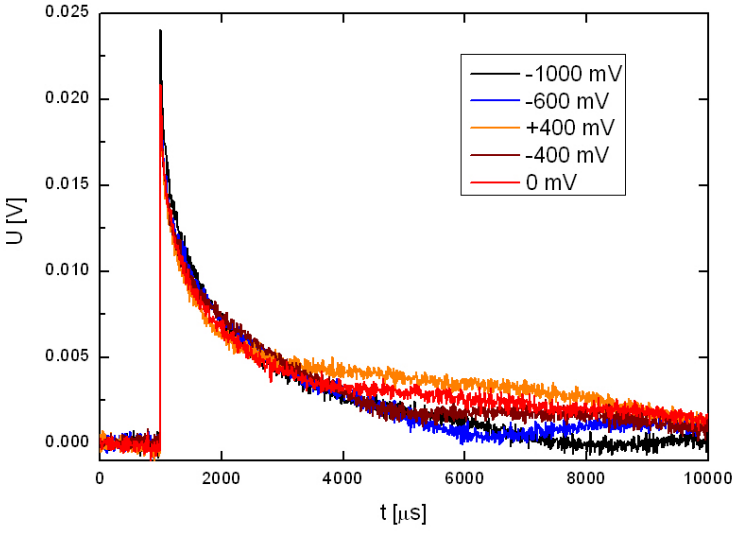

A2 Samples photo-voltage spectra

Photo-voltage responses of the samples right after their preparation and one month later at different time scales. The signal of the reference samples is reported for comparison.

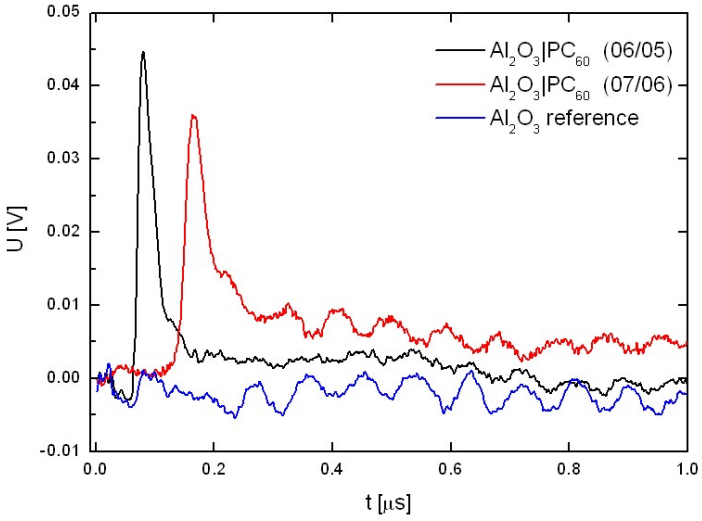

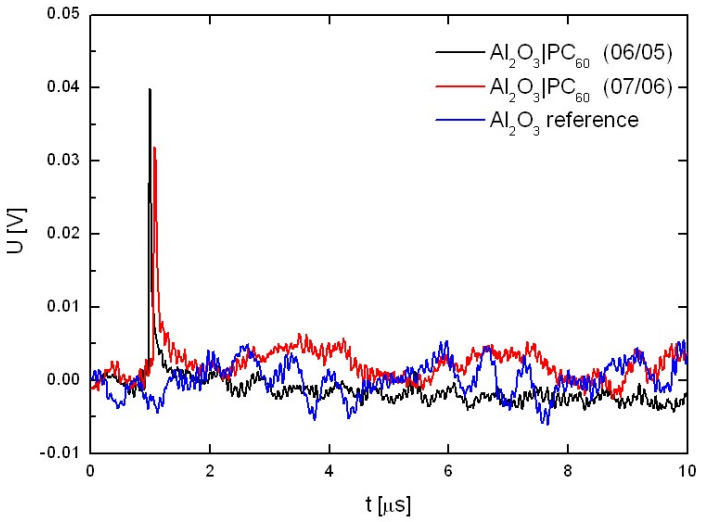

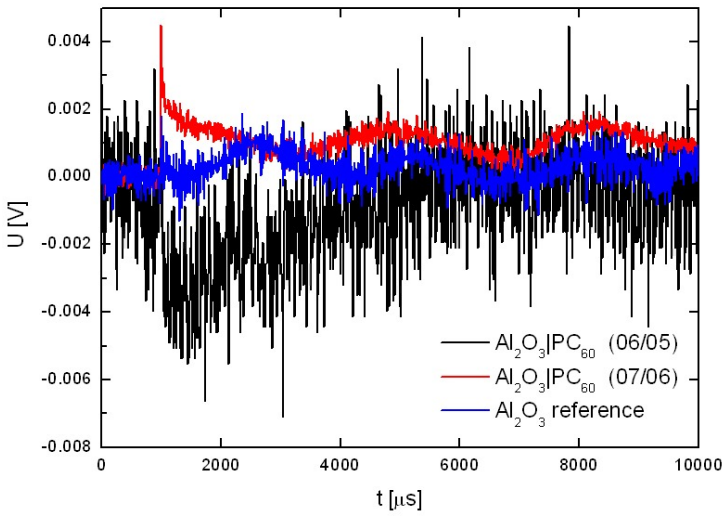

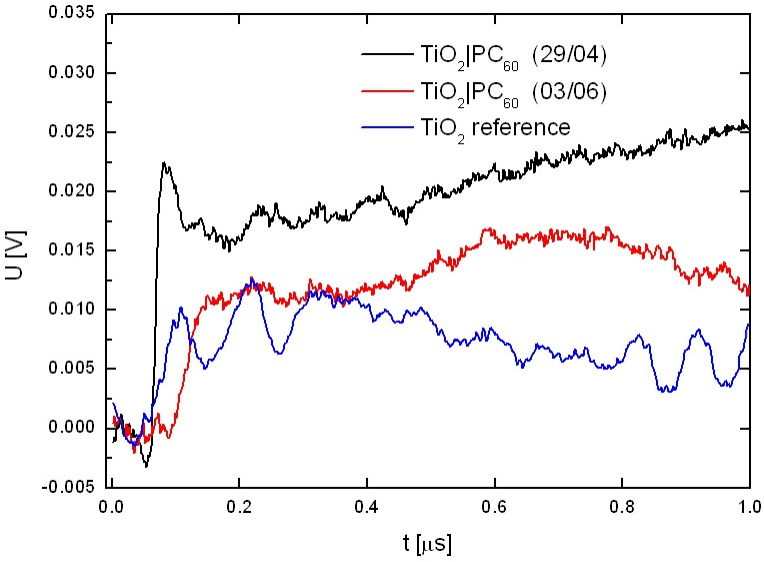
TiO2|PC60 (29/04)
TiO2|PC60 (03/06)
TiO2 reference
U [V]
t [µs]

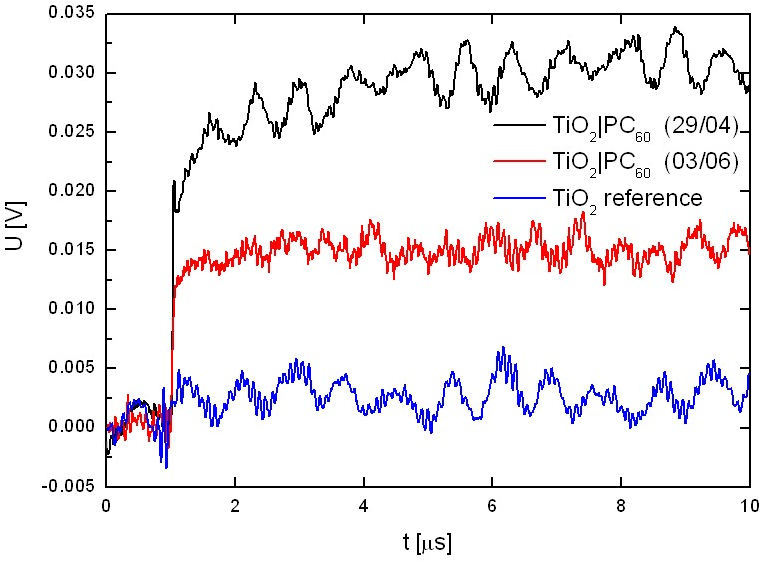
TiO2|PC60 (29/04)
TiO2|PC60 (03/06)
TiO2 reference
U [V]
t [µs]

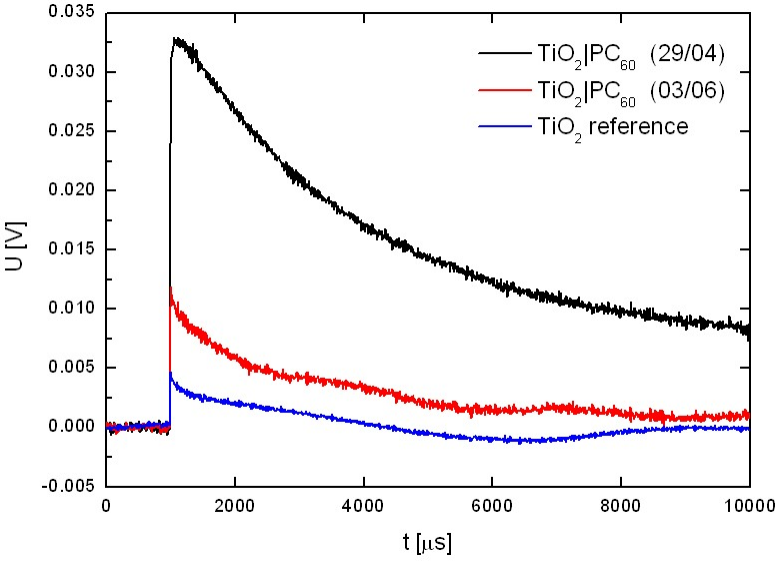
TiO2|PC60 (29/04)
TiO2|PC60 (03/06)
TiO2 reference
U [V]
t [µs]

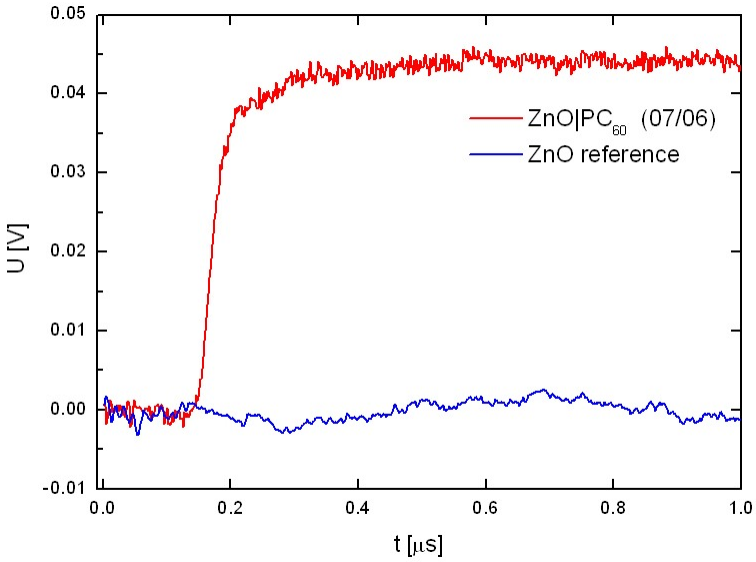
0.05
0.04
0.03
0.02
0.01
0.00
-0.01
U [V]
0.0
0.2
0.4
0.6
0.8
1.0
t [µs]
ZnO|PC60 (07/06)
ZnO reference

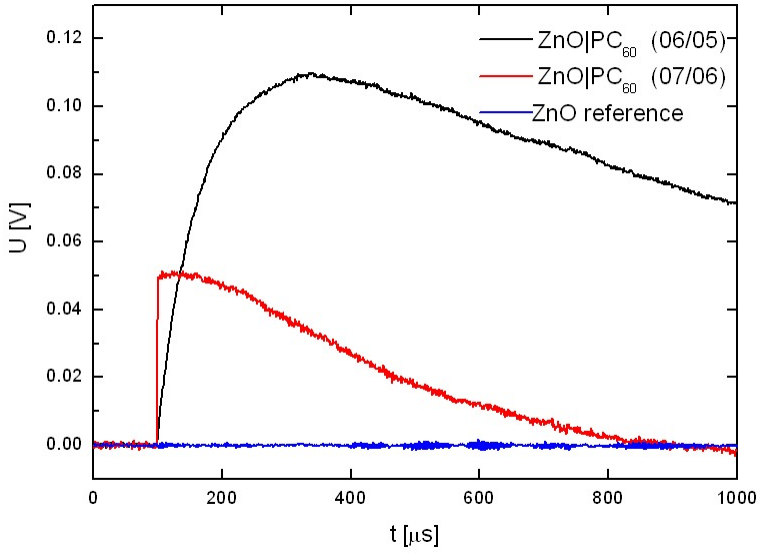
0.12
0.10
0.08
0.06
0.04
0.02
0.00
U [V]
0
200
400
600
800
1000
t [µs]
ZnO|PC60 (06/05)
ZnO|PC60 (07/06)
ZnO reference

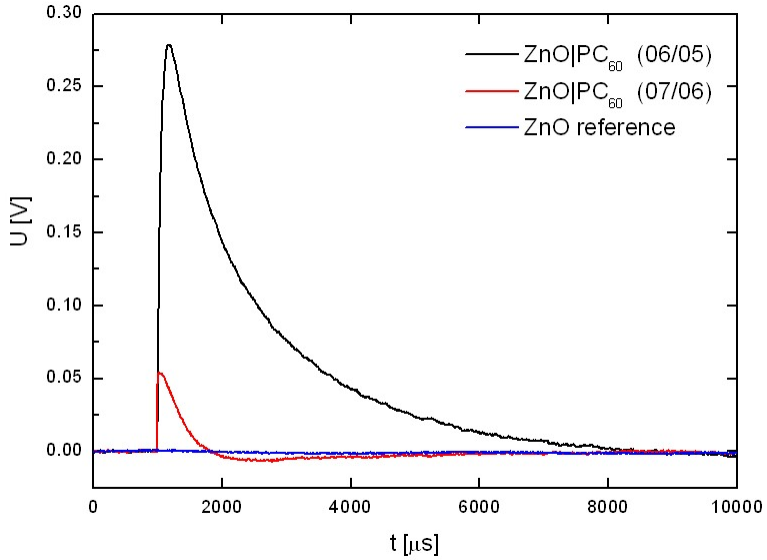
0.30
0.25
0.20
0.15
0.10
0.05
0.00
U [V]
0
2000
4000
6000
8000
10000
t [µs]
ZnO|PC60 (06/05)
ZnO|PC60 (07/06)
ZnO reference

A3 Samples absorption spectra

Absorption spectra of photo-voltage samples before, black line, and after, red line, the TRMDC measurements.